The Evolution of Mass Spectrometers for High *m/z* Biological Ion Formation, Transmission, Analysis and Detection: A Personal Perspective

Iain D. G. Campuzano[1]* and Joseph A. Loo[2]*

1. Large Molecule Discovery and Research Data Science, Amgen Research, Amgen, Thousand Oaks, California, 91320, USA

2. Department of Chemistry and Biochemistry, Department of Biological Chemistry, University of California-Los Angeles, Los Angeles, California 90095, USA

*Corresponding authors iainc@amgen.con and jloo@chem.ucla.edu

Abstract

Mass spectrometry (MS) has become an essential tool in virtually all academic, pharmaceutical and biopharmaceutical analytical laboratories. The specialized and bespoke area of MS research and application of high *m/z* ion (>*m/z* 6,000 and high mass, >150 kDa) formation, transmission, analysis and detection is a relatively new area of focus for MS, that has seen dramatic acceleration in interest over the last two decades. Herein we delve into this exciting aspect of MS, discussing how MS instrumentation has been refined and evolved for native-MS analysis. We cover the early groundbreaking experiments showing high *m/z* ion formation, transmission and preservation of protein structure in the gas phase. Additionally, we discuss specific instrument optimizations and modifications that have advanced high *m/z* generation, transmission, analysis and detection, contributing to the research area known as gas-phase structural biology. Native-MS sample introduction methods, emerging technologies, and future perspectives are also examined. Finally, we share personal opinions, observations and experiences that are new to the community or previously unpublished.

Introduction

Mass spectrometry (MS) is as ubiquitous as the application of nuclear magnetic resonance [1], surface plasmon resonance [2] and multiple chromatographic analytical methods [3] for analytical project advancement. MS is routinely used in pharmaceutical [4] and biopharmaceutical settings [5, 6] including, but not limited to, research [6, 7], development and lot release [8 9], government research [10] and academic research [11] across the globe. MS has become much more routine, useable and accessible as a result of many factors, such as massively reduced instrument footprint, multiple detector types, easy and routine software control, much of which has been MS manufacturer driven. And of course, the development of both matrix-assisted laser desorption ionization (MALDI [12]) and electrospray ionization (ESI [13 14, 15]) which enabled the generation of biological ions, subsequent detection and exquisite characterization by the MS technologies described herein.

In the context of this discussion, what is high *m/z*? This question really depends on one's perspective. If one's research area is Inductively Coupled Plasma MS [16] where the *m/z* range is typically no higher than *m/z* 250, then arguably a peptide of molecular weight (MW) 1500 Da, such as Glu-Fibrinopeptide b with an *m/z* value of 785.8 $[M+2H]^{2+}$, or routine reversed phase tandem-MS proteomics applications [17] can be considered high *m/z*. However in realistic terms, ions above the typical upper *m/z* range of a quadrupole instrument (generally is *m/z* 2000 [18]) and are routinely accessible by ToF [19], orthogonal acceleration ToF (oa-ToF [20]) and Fourier transform ion cyclotron resonance (FT-ICR [21]) were and are considered to be high *m/z*.

Over the past four decades the *m/z* and MW limits of MS instruments have been pushed (higher) and therefore have continually evolved. One can argue that the main impetus for this MS evolution was due to the need to analyze biological molecules that retain their native-like tertiary and quaternary gas-phase structures, being electro-sprayed directly from aqueous based solutions in to the vacuum of the MS. Exactly two decades ago, the term native-MS was coined [22], and the research area of gas-phase structural biology was born [23]. For a number of excellent reviews of native-MS and structural biology, we point the authors to the following review articles by Loo [24], van den Heuvel and Heck [22], Benesch [25], Benesch and Ruotolo [26] Benesch and Hilton [27] and Olinares [28]

For native-MS and gas-phase structural biology to have evolved to where it is today, MS instrument developments needed to be realized, implemented and become readily available for use by the diverse range of MS researchers across the globe. MS technology has evolved through multiple key areas, which we will discuss in detail below. For brevity, high *m/z* inorganic ion detection by FT-ICR and ion trap, the first proteins to be electro-sprayed from aqueous based solutions to bespoke time-of-flight (ToF) and Orbitrap MS instrumentation enabling mega-Dalton virus detection, are all key progress milestones. Herein we have chosen to focus on the enabling technology, that is MS instrument evolution affording high *m/z* and high MW formation, transmission and detection, that has enabled the area of native-MS.

This is not intended to be an exhaustive literature review. Instead, it's a personal perspective and commentary on subject matter that we are both passionate about and based on the works that we feel are most representative, impactful, and influential in high *m/z* and high MW research spanning the past four decades. Finally, additional authors' opinions on related topics can also be found in the Supporting Information.

What was High *m/z* Analysis?

Early pioneering high *m/z* research was presented by Amster [29] and Lebrilla [30] where they demonstrated, using cesium desorption ionization [31], the transmission and detection of CsI clusters at *m/z* values 16,241.9 $[Cs(CsI)_{62}]^+$ and 31,8331.6 $[Cs(CsI)_{122}]^+$ respectively, by FT-ICR MS (Figure 1a) and Kaiser [32] measuring *m/z* 44,560 $[Cs(CsI)_{171}]^+$ by quadrupole ion trap MS (Figure 1b). In 1983, Barber produced an $[M+H]^+$ spectrum of proinsulin (MW 9.4 kDa) on a ZAB-HF tandem magnetic and electric sector mass spectrometer [33] using fast atom bombardment (FAB [34]). ^{252}Cf-plasma desorption [35] coupled to ToF was an effective ionization technique for high *m/z* biological molecule analysis, where porcine pepsin was observed over a narrow set of charge states $z = 4^+$ to $z = 1^+$, up to *m/z* 34,633 for the $[M+H]^+$ ion [35, 36] (Figure 1c; which can still be classed as high *m/z* today!). In the early 1990s, MALDI ToF was widely adopted for high *m/z* analysis of large biomolecules. Nelson [37] demonstrated this when they reported the analysis of an intact IgM pentamer, with a measured MW of 982 kDa, with observed charge states ranging from $z = 6^+$ to $z = 2^+$. The development of ESI, specifically in combination with oa-ToF, further revolutionized the field of high *m/z* analysis.

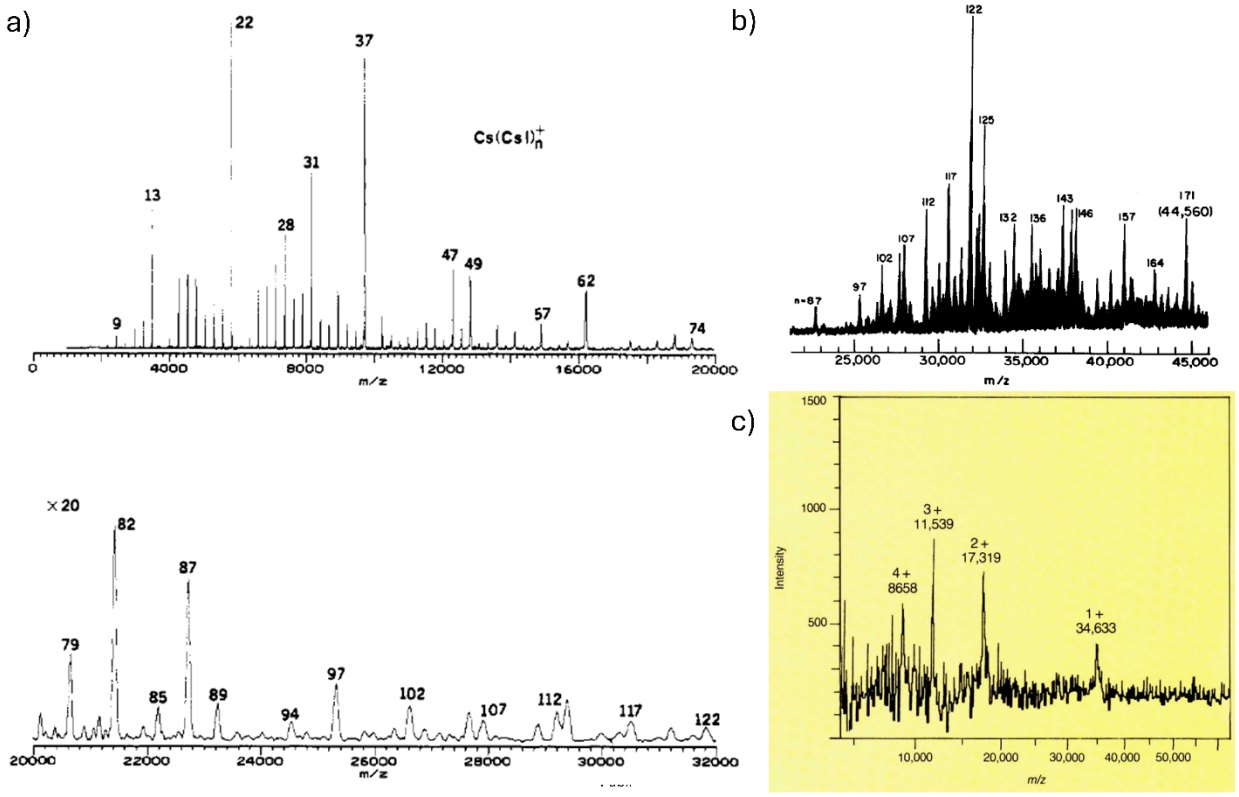

Figure 1. Examples of high *m/z* examples a) cesium iodide cluster ions obtained with an external ion source FT-ICR MS. The peaks are labeled by the number of cesium iodide units in the cluster, according to the general formula $[Cs(CsI)_n]^+$, reproduced from reference [30], with permission from the American Chemical Society, Copyright 1990; b) a high *m/z* cesium iodide spectrum using an axila modulation frequency quadrupole ion trap with reduced drive frequency, reproduced from reference [32] with permission from Elsevier Publishers, Copyright 1991; c) a plasma desorption mass spectrum of porcine pepsin obtained on a BIO-ION 20, reproduced from reference [35] with permission from the American Chemical Society, Copyright 1988.

The Early Days of Intact Protein Analysis

After the initial discovery that ESI could generate measurable ions from protein solutions without causing significant fragmentation, a hallmark of electron ionization and FAB ionization methods, there was a mild "race" to demonstrate desorption/ionization of larger molecular mass proteins. Early ESI measurements of proteins such as serum albumin (66 kDa) and its covalent dimer (133 kDa) were measured using quadrupole [38] and quadrupole ion trap [39] mass analyzers.

The initial "native" mass spectra of human FKBP with FK506 and rapamycin complexes published by Ganem and Henion [40] and the myoglobin-heme complex by Katta and Chait [41] (Figures 2a & b) also used a quadrupole analyzer. ESI coupled to quadrupole ion traps were quickly developed as a viable detector for protein MS. Later, other higher-performance analyzers, such as ToF [42, 43] (catalase HP II) and FT-ICR [44] (tetrameric streptavidin) were demonstrated to have capabilities to measure protein ions high on the *m/z* scale. Even the magnetic sector instrument, once considered the premier mass spectrometer for protein sequencing applications [45], pioneered by Klaus Biemann, was interfaced with an ESI inlet. Figure 2c shows ESI mass spectra of a FabI (enoyl acyl carrier protein reductase) homotetramer complex measured with a Finnigan MAT900 magnetic sector instrument [46]. Analysis of alcohol dehydrogense under native-MS conditions has also been demonstrated using a magnetic sector MS [47].

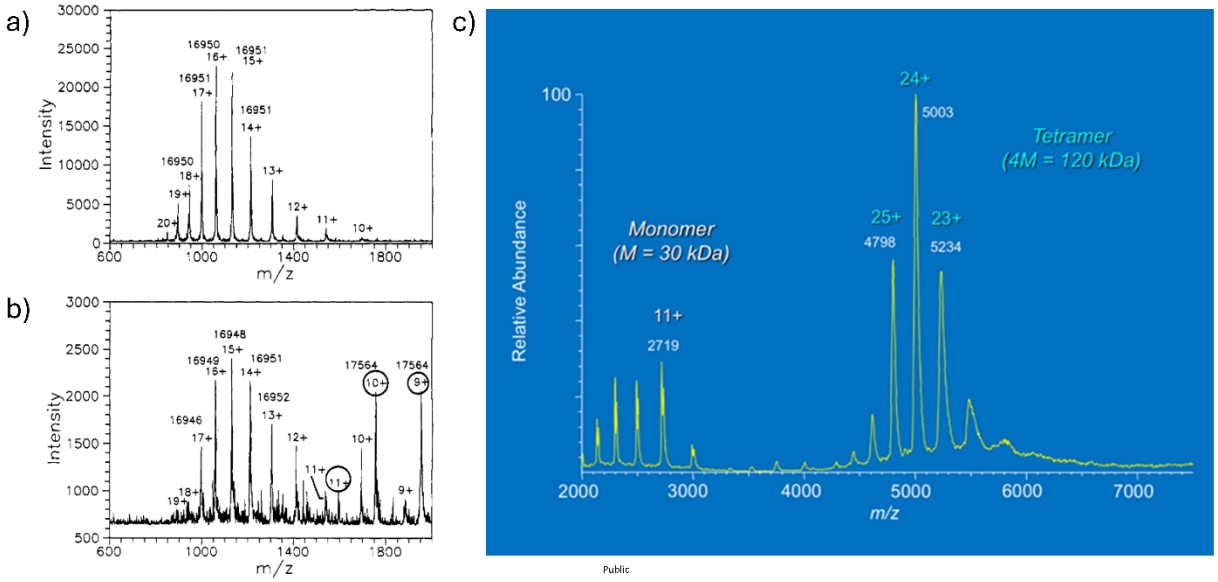

Figure 2. Early examples of native-MS analysis of: a) myoglobin (30-40 μM) acquired at pH 3.35; b) myoglobin (30-40 μM) acquired at pH 3.90, using a quadrupole MS, reproduced and modified from reference [41] with permission from the American Chemical Society, Copyright 1991; c) enoyl acyl carrier protein reductase (FabI) homotetrameric protein complex acquired on a double focusing magnetic sector MS (Finnigan MAT 900) reproduced from reference [46].

Noncovalent Complexes become Larger and *m/z* Values Higher

Several pivotal works in ionization, instrument development and applied high *m/z* (and high MW) analysis will now be briefly described. Mann and Wilm initially described nanoESI (nESI [48, 49]) affording gentle aqueous to gas-phase transfer and desolvation of small droplets containing proteins and associated complexes. From an MS instrument perspective, the notably unmodified "off the shelf" first generation Micromass quadrupole time-of-flight (Q-ToF [50] [51]) and the Micromass LCT (non-quadrupole based ToF [51]) from the late 1990s afforded routine high *m/z* analysis,

Tito and Robinson [52] described the analysis of the tetradecameric chaperone complex, GroEL (14mer, 802 kDa). The analysis was performed on a non-modified first-generation Q-ToF [50, 51], where the source pressure was increased (Figures 5a & b). The resulting spectrum displayed partially resolved charged states observed at *m/z* 10,000 (Figure 3a). It must be noted that this GroEL sample was nESI sprayed from a pH 5 water solution, as ammonium acetate was not commonly used then.

The next was by Rostom where they analyzed intact 30S, 50S and 70S intact ribosome complexes [53]. In 2000, Tito [54] published a spectrum of an intact virus of MW 2.5 MDa acquired on an LCT ToF MS instrument [51].

Over the subsequent five years, instrument modifications (described below) were realized and implemented, allowing for dramatically improved high *m/z* (and high MW) transmission. As a result, improved GroEL charge state separation was rapidly achieved (Figure 3b). Finally, over the past quarter of a century, GroEL has taken on legendary status for native-MS analyses, in that it's now considered a "yardstick" protein standard, by many groups, for instrument evaluation [55-58]. It is important to note that in addition to an optimized MS instrument, the key to a well-

resolved GroEL native-MS spectrum is a sample preparation method specific for this complex [59, 60].

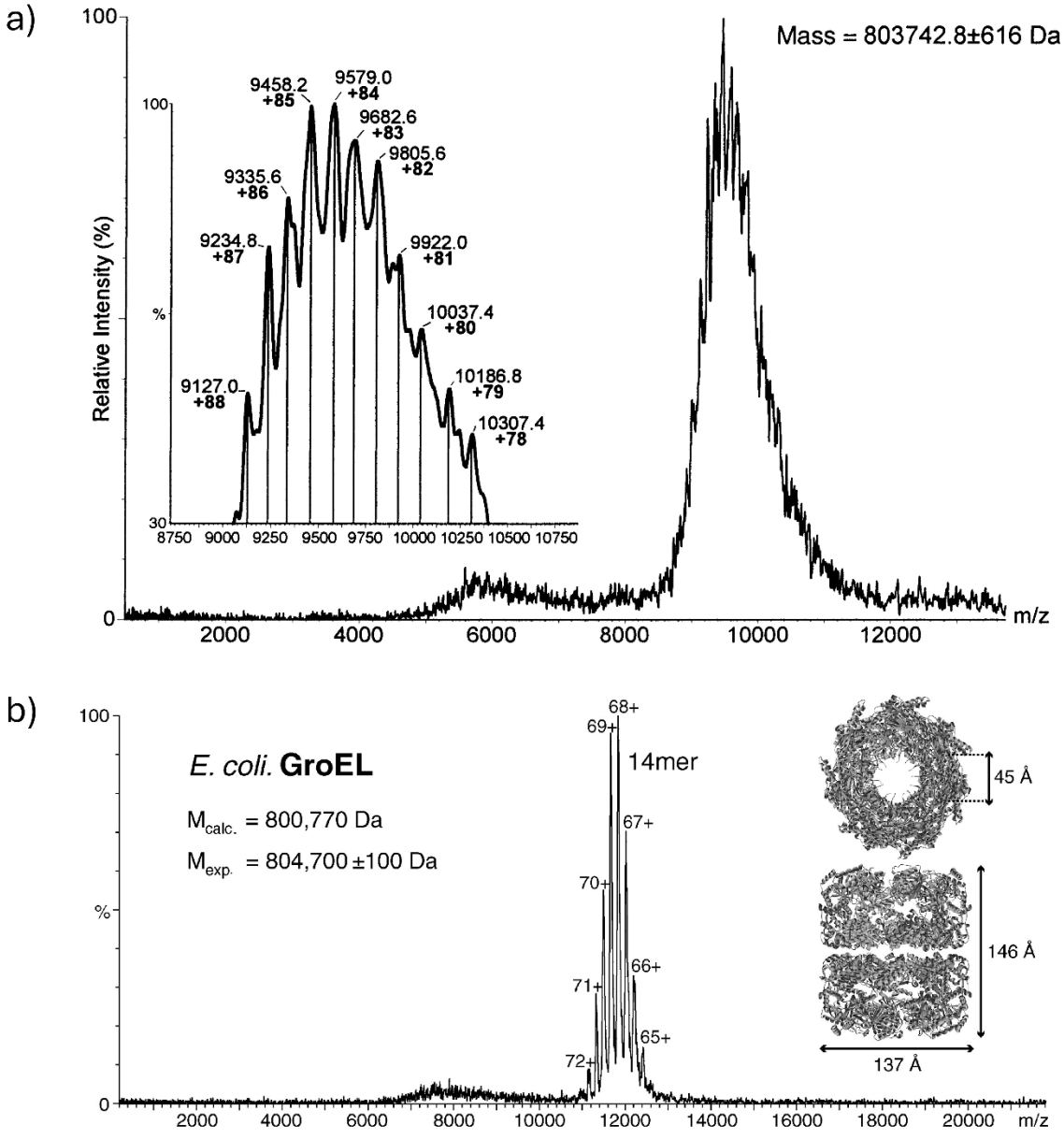

Figure 3. The evolution of GroEL native-MS over five years: a) the first published GroEL spectra, acquired on a non-modified Q-ToF MS, reproduced from reference [52] with permission from the American Chemical Society, Copyright 1999; b) the first published close-to-baseline resolved GroEL charge states acquired on a modified Q-ToF MS, reproduced from reference [61] with permission from Elsevier Publications, Copyright 2004.

What is High *m/z* Now?

The development of ESI [13, 14, 62] rapidly afforded more routine analysis of higher *m/z* species, especially when combined with oa-ToF analyzers, that operate at relatively high pressures (compared to the ICR and Orbitrap) with routine extended *m/z* ranges In the context of this manuscript, high *m/z* has somewhat moved away from the ultra-high *m/z* CsI spectra acquired prior to the development of ESI, tohigh quality charge state separation of native proteins and protein-protein complexes afforded by the instrumentation and associated development described herein. As a protein or protein complex becomes larger and is no longer solubilized in an acid and organic mobile phase, but is solubilized in an aqueous-based solution that is close to neutral pH, such as ammonium acetate (typically 50-200 mM or higher, depending on sample[63 64]) it retains a more native-like folded structure, therefore possesses less overall surface charge (*z*), therefore appearing higher up the *m/z* scale.

High *m/z* analysis is now more routine than what it was two decades ago and in the context of protein analysis, has evolved into its own research a field that can broadly be termed as native-MS [22, 65] or even gas phase structural biology [23]. The diversity of samples analyzed by researchers in these areas is now vast and range from monoclonal antibodies (mAbs) to membrane proteins and beyond, being analyzed in both positive and negative nESI polarities (Figures 4a-f).

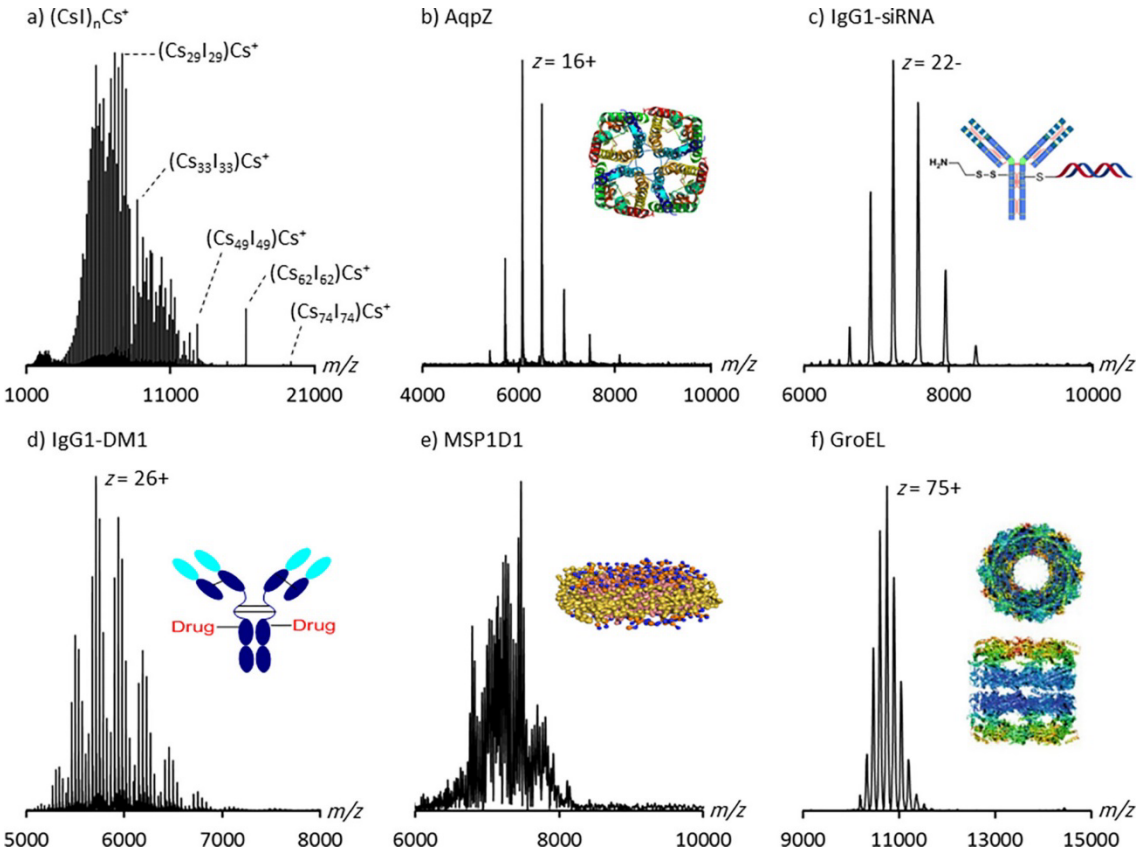

Figure 4. A selection of inorganic salt clusters, proteins and proteins complexes, analyzed by nESI, displaying charge states over a wide *m/z* range, acquired on a solariX 15 Tesla FT-ICR MS. All data displayed in magnitude mode using the Hann windowing function of $F = 0.5$: a) cesium iodide at a concentration of 50 µg/µL; b) the tetrameric AqpZ complex liberated fromC8E4-micelles, 10 µM (1RC2, downloaded from www.rcsb.org); c) an IgG1-siRNA conjugate, 5 µM (displaying a single cysteamine modification); d) an IgG1–DM1 conjugate, 5 µM; e) the empty MSP1D1 nanodisc, 10 µM and f) the tetradecameric chaperone complex GroEL, 5 µM (4V43, downloaded from www.rcsb.org). Reproduced from reference [57] with permission from the American Chemical Society, Copyright 2020.

Bespoke MS Instruments make a Big Difference

A number of key reports have documented [66-68] and patented [69, 70] the bespoke modifications required for improved high *m/z* and high MW transmission and detection. We will now discuss each MS region, adding additional, and in certain cases, rarely referenced work.

Increasing Source Pressure: Ions are transferred into the intermediate pressure region of the MS source by a combination of gas flow, vacuum and voltage potential differences. Once inside the intermediate pressure region of the source, there is a free jet expansion process [71]. This process results in the ions significantly deviating from their original axial and radial trajectories and gaining energies of 1 keV (or higher) with initial axial and radial velocities in the order of 2000 m/s and 1000 m/s, respectively [43], depending on the size of the complex being studied.

The first documented uses of increased source pressure for improved high *m/z* transmission were by Krutchinsky [43], Rostom [52] and Schmidt [72]. In 2001 Tahallah [73] systematically described the adjustment of the Micromass LCT Z-Spray source backing pressure for optimal high *m/z* transmission, for the protein complex vanillyl alcohol oxidase. This is a very simple, yet a highly effective MS source modification, where the external rotary pump was restricted by closing a factory, or user installed, restriction valve (Edwards Speedivalve; Figures 5a&b). The effect was an increase in pressure (~2 mbar to ~7 mbar) in the intermediate region of the Z-Spray source; the region immediately between the sample cone and extraction cone. This increase in source pressure provided the required collisional damping/cooling [43, 67, 68] and focusing of the large energetic ions, resulting in improved transmission, and ultimately, their detection. The pressure was accurately monitored by means of an Edwards pirani gauge [73].

Other early examples of increasing Z-Spray source pressure are described by Sobott [61, 66]. Campuzano [70, 74] also described how heavy polyatomic gases, such as sulfur hexafluoride (SF_6) and octafluoropropane (C_3F_8), when used as a source cone curtain gas, are effective modifications for improving high *m/z* transmission. Bagal [75] also demonstrated the use of xenon (Xe) and SF_6 as a cone gas for stabilizing small non-covalent complexes. It is likely that these large mono and polyatomic cone gases are carried into the intermediate pressure region of the Z-Spray source where they have the effect of collisionally cooling [67, 68] large energetic ions.

Additional pressure increases in the immediate proceeding ion optics regions have been implemented. These were achieved by direct introduction of gases (argon, Ar or nitrogen, N_2) into the source multipole (quadrupole or hexapole) region of the Q-ToF MS instrument [66, 67]. A gas flow restrictive sleeve [67, 68] (32 mm id and 100 mm in length) was also placed over the hexapole ion optics (Figure 5a) that increased the local pressure, improving CsI cluster [67], proteasome 20S [67] and GroEL [68] transmission. The ion sleeve pressure was not adjustable.

Transmission is increased due to the improved axial and radial focusing, described by Chernushevich [67] and later by van den Heuvel [68] Benesch [25] and Lee [76], whereby the stopping path (for proteasome 20S) was reduced to approximately 120 mm at $4e^{-2}$ mbar (Figure 5c). Radio frequencies were also optimized in these regions to favor high *m/z* transmission. For example, the Synapt G2 [77, 78] (*circa* 2010 Waters Corporation, MS Technologies Center) can utilize a maximum radio frequency (RF) peak-to-peak voltage of 450 V at a frequency in the 1-3 MHz range, applied to the source stacked ring ion guide [79].

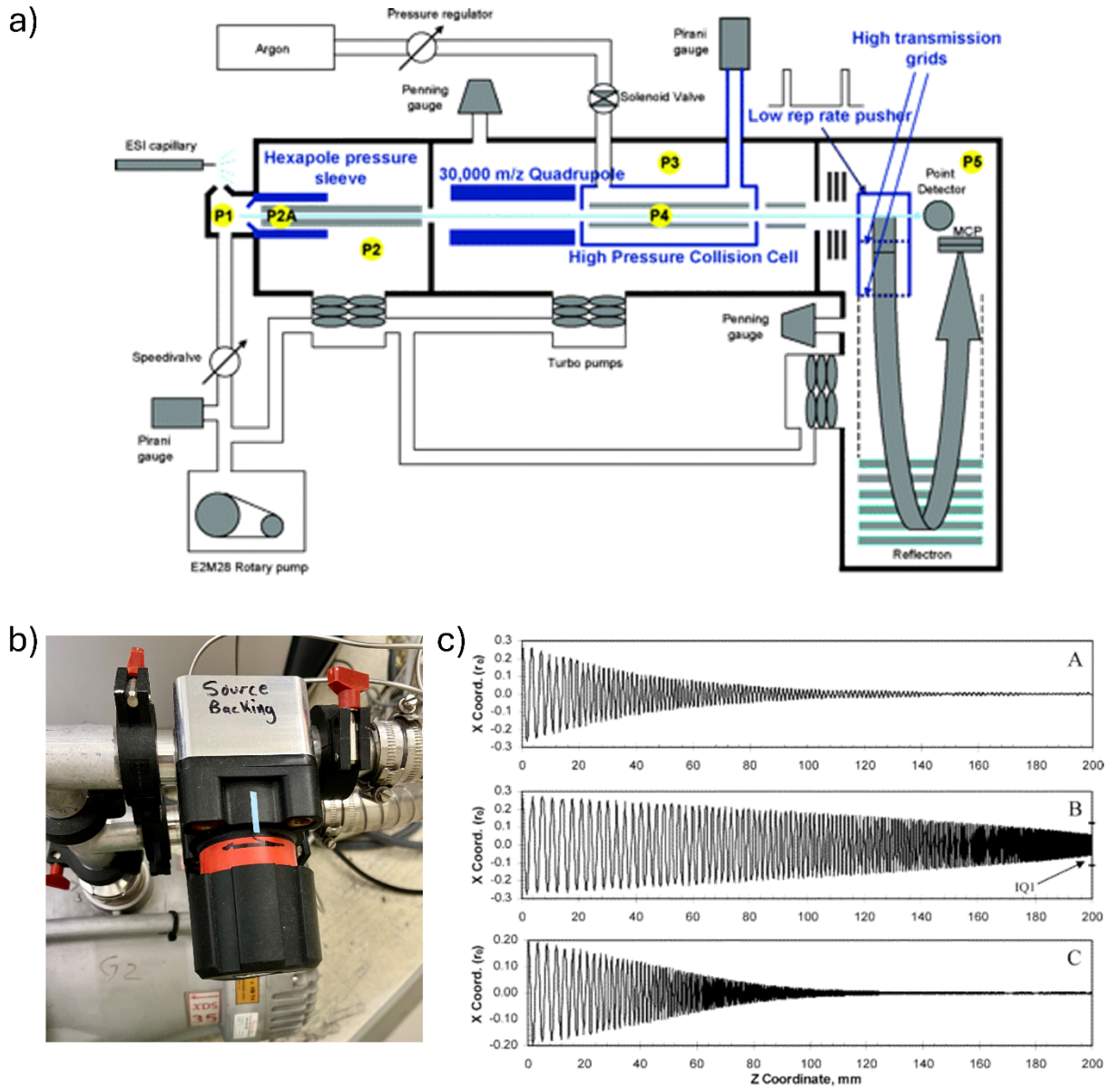

Figure 5. Early bespoke Q-ToF ion optics modifications to enhance high *m/z* ion transmission: a) a Micromass first generation Q-ToF MS instrument schematic describing the important modifications for improved high *m/z* transmission, reproduced from reference [68] with permission from the American Chemical Society, Copyright 2007; b) arguably one of the most effective modifications to the Micromass-Waters Z-Spray source to enable high *m/z* transmission, the Edwards speedi-valve used to restrict source pumping, and increase localized pressure. The current image is of a speedivalve mounted to a Waters Synapt G2 and an Edwards XDS 35 scroll pump; c) the simulated ion stopping paths for myoglobin at $1e^{-2}$ mbar (A); proteasome 20S at $1e^{-}$

^{2} mbar (B) and proteasome 20S at $4e^{-2}$ mbar (C), reproduced and modified from reference [67] with permission from the American Chemical Society, Copyright 2004.

Low Frequency Quadrupole RF-Generators: The quadrupole serves two purposes within an MS instrument; to transmit ions in RF-only mode and for ion (*m/z*) selection. As proteins and protein complexes become larger (in MW, when compared to monomeric cytochrome-C and myoglobin) and when ionized, by nESI, from neutral aqueous solutions, the charge states appear higher on the *m/z* scale. As a result, MS ion optics optimization was required.

Prior to the field of native-MS fully establishing itself, multiple studies were conducted where the upper *m/z* selection range of a quadrupole were increased to *m/z* 8585 [80], 9000 [81] and 45,000 [82]. When operating in RF-only (transmission) mode, the upper *m/z* limit is determined by Equation 1 [83]:

$$m/z_{\max} = \frac{4eV_{\mathrm{RFmax}}}{0.70600 r_0^2 \Omega^2} \qquad (1)$$

where *e* is the electronic charge of an electron in Coulombs ($1.602e^{-19}$), V_{RFmax} is the maximum RF voltage output applied to adjacent quadrupole rods. r_o is the field radius, which is the center point of the quadrupole to an electrode. Ω is the operating frequency and 0.70600 is the q_x value from the Mathieu equation first stability region [83].

Sobott described the reduction in RF frequency, from 832 kHz to 300 kHz allowing for an 8-fold extension in quadrupole selection ability (*m/z* 4190 to 32,400) and based on known quadrupole RF-transmission behavior, up to five times (Figure S1, Supporting Information) the RF-specified *m/z* transmission can be achieved, which in practical terms, is in excess of *m/z* 90,000. It must also be noted that CsI high *m/z* transmission was demonstrated on an unmodified 15 Tesla FT-ICR MS using a 6 k quadrupole (Figure 4a [57]). Sobott [66] exquisitely demonstrated CsI *m/z* 22,226 (CsI cluster $[CsI_{85}]Cs^{+}$) quadrupole selection (Figure 6a). Aquilina [84] reduced the complexity of a highly polydisperse alpha crystallin complex, by *m/z* 10,000 selection and subsequent collisional activated dissociation (CAD). Uetrecht [85] demonstrated tandem-MS at *m/z* 21,000 for the HBV

cp149 capsid. Campuzano [86] also demonstrated how tandem-MS of the highly polydisperse nanodisc, followed by mild CAD (and infrared multiphoton dissociation; IRMPD) on an FT-ICR MS, can be used to dramatically simplify the spectra, affording manual charge and MW assignment (Figures 6b & c). High *m/z* quadrupole selection has also been demonstrated on the hexameric membrane protein CYP3A4 [87]. Finally, the extended *m/z* range Orbitrap QExactive described by Belov [56], contained a quadrupole operating at 285 kHz, demonstrating *m/z* 10,265 (CsI cluster $[CsI_{39}]Cs^+$) selection.

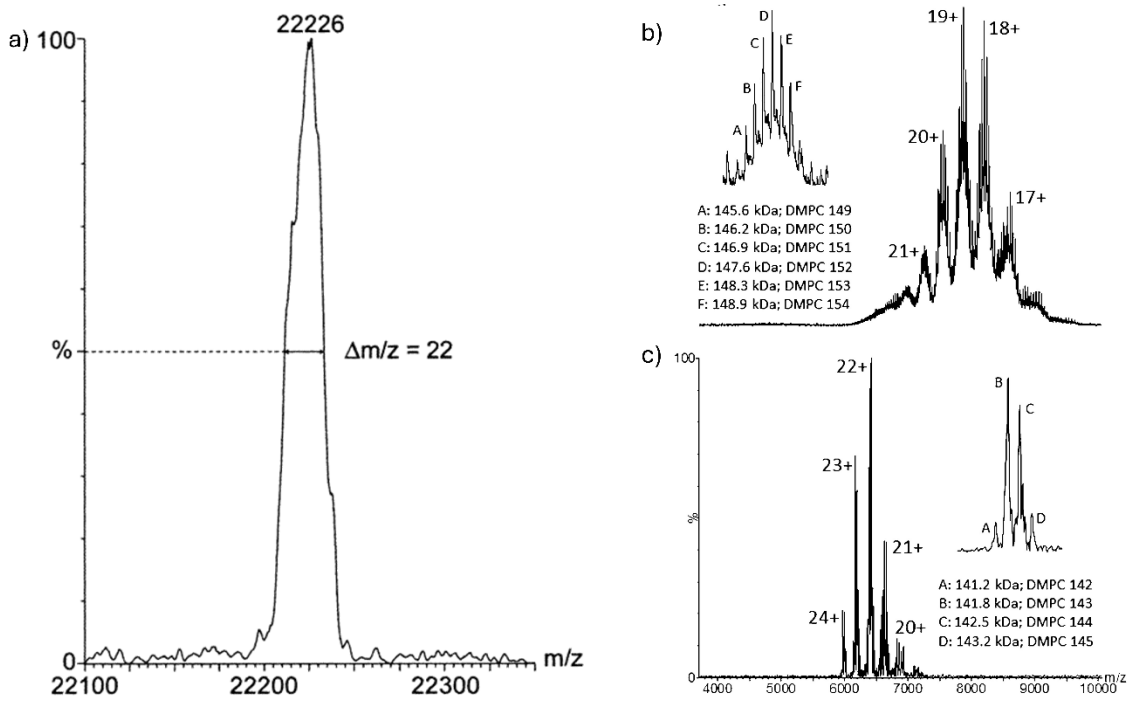

Figure 6. Examples of Q-ToF and FT-ICR high *m/z* quadrupole selection: a) cesium iodide cluster $[CsI_{85}]Cs^+$ at *m/z* 22,226, reproduced from reference [66] with permission from the American Chemical Society, Copyright 2002; b) nanodisc spectral simplification by collision activated dissociation, Q-ToF Trap TWIG 40 V, SF_6; c) 15 Tesla FT-ICR infrared multiphoton dissociation, 0.2 s, 50% power, Synrad 10.6 μm CO_2 laser, reproduced and modified from reference [86] with permission from the American Chemical Society, Copyright 2016.

The Collision Cell: A critical component for high *m/z* transmission, and optimal tandem-MS is the collision cell and the gas that is utilized. Briefly, CAD was first described Jennings [88] in 1968, using an MS9 double focusing mass spectrometer (Associated Electrical Industries, Ltd.). In the context of high *m/z* transmission and specifically native-MS, different gases have been used, ranging from small monoatomic to larger polyatomic molecules (Table 1).

In 1988, Schey [89] described multiple collision gases including, but not limited to helium, neon, Ar and Xe, for small molecule (=< 352 Da) CAD purposes. This work preceded any biologic high *m/z* transmission and associated MS or tandem-MS optimization, using monoatomic and polyatomic collision gas studies by over a decade. In the context of the early Q-ToF MS instrument and associated high *m/z* transmission, the presence of a collision cell filled with a high-pressure neutral gas is absolutely essential for the required collisional cooling [67, 68] of the large energetic ions, minimizing or completely eliminating ion losses prior to the orthogonal injection pusher stack, thus enabling their subsequent analysis and detection by oa-ToF and microchannel plate, respectively.

The effect of collision cell voltage is also described by Green [90] and van den Heuvel [68] demonstrating fine structure, representing hemoglobin subassemblies and detection of noncovalently bound flavin cofactor, respectively. A consequence of operating at higher collision energies is that the ions become more energetic, requiring a higher collision cell gas pressure to refocus and cool them. To increase the localized gas pressure (in the collision cell) the apertures of the collision cell entrance and exit lenses were reduced from a diameter of 2.4 mm to 1.6 mm ($2e^{-3}$ to $1e^{-2}$ mbar and $5e^{-3}$ to $2e^{-2}$ mbar, Ar) [67]. Collision cells also evolved from hexapole ion guides to stacked ring ion guides (SRIGs [79]). This change did not impact high *m/z* transmission, as demonstrated by multiple groups [77, 91-93]. Additional declustering and desolvation can also be achieved in the SRIG collision cell of an MS instrument. This has been effectively demonstrated on GroEL [60], where GroEL charge state FWHM was dramatically reduced as collision energy increased (50-200 V, using SF_6 as the collision gas).

The nature of the collision gas is important. The first description of the use of Xe and SF_6 for native-MS applications was by Tito [69] and then Sobott [61]. Lorenzen [94] described how the molecular nature of the collision gas (monoatomic noble gas-based) is also critical. The effect of the collision gases (Ar, Krypton; Kr, Xe) were measured as a function of transmission and

therefore, detection of the CAD-induced GroEL dodecamer (12-mer) decomposition species. The larger collision gas, Xe, was the most effective. The use of Xe as the high energy collision activated dissociation (HCD) gas in the Orbitrap (and N_2) was also described by Rose [55]. Due to the higher number of degrees of freedom (*3N;* translational, rotational and vibrational; Table 1), polyatomic molecules make for more optimal MS collision gases. Their increased ability to absorb the kinetic energy of translational motions of the highly energetic macromolecular ions and dissipate this energy equally across all degrees of freedom [69, 89], resulting in reduced fragmentation [89], improved MS and tandem-MS transmission and ultimately detection [94]. One must also note that as the collision gas MW increases (and degrees of freedom) the polarizability constant also increases (Table 1). One can therefore hypothesize that the increased polarizability constant of the collision gas results in a stronger long-range ion-induced ion-neutral dipole interaction, which also contributes to improved high *m/z* focusing, transmission and the overall collisional cooling process.

Collision Gas	**MW** (Da, ave)	**Degrees of Freedom Total***	**Polarizability Constant** ($x10^{-24}$ cm^3)	**Additional Notes**
Argon (Ar)	39.9	3	1.64 [95]	Originally described by Morris [50] for Q-ToF tandem-MS. Later described by Lorenzen [94] for GroEL tandem-MS optimization
Krypton (Kr)	83.8	3	2.48 [95]	Described by Lorenzen [94] for GroEL Q-ToF tandem-MS optimization
Xenon (Xe)	131.3	3	4.04 [95]	Described by Tito [69] and Sobott [61] (Q-ToF) and later by Lorenzen

				[94] for GroEL Q-ToF tandem-MS optimization.
Nitrogen (N_2)	28.0	6	1.74 [95]	Described by Tito for collisional cooling in intermediate pressure region of an LCT ToF MS [54]. Described by Rose [55] for GroEL (Orbitrap-EMR) and by Belov [56] for GroEL and Pyruvate Kinase tandem-MS (in HCD cell)
Sulphur Hexafluoride (SF_6)**	146.1	21	6.54 [95]	Described by Tito [69] and later in publications by Ruotolo [92] and Campuzano [60] (all Q-ToF)
octafluorocyclobutane (cC_4F_8)	200.0	36	7.37-12.47 [96]	Described by Campuzano [97, 98] for mAbs, mAb-siRNA conjugates, nanodiscs and GroEL (Q-ToF)

Table 1. A table describing the collisional cell gases that have been used over the past 30 years for either high *m/z* transmission or protein complex tandem-MS. The collision gas MW was calculated using MassLynx v4.1 (Waters MS Technologies, Manchester, UK). *Degrees of freedom based on 3 total (translational only) for monoatomic and 3*N* total (3 translational, 3

rotational and 3*N*-6 vibrational) for non-linear polyatomic gases. *N* is equal to the number of atoms. **SF_6 is a potent greenhouse gas [99].

General Ion Declustering Considerations: The term declustering refers to the removal of non-covalently associated solvent, salt molecules and counter ions that were not removed from the protein or protein complex, during the nESI process. These species add to the charge state peak width [100] and can be removed by increasing the number of ion-neutral collisions within the MS, by increasing acceleration voltage in a number of different areas in the MS.

In the Z-Spray source the voltage offset between the atmospheric sampling cone and partial vacuum region (~6-7 mbar) and extraction cone can be increased to 200 V resulting in increased ion-neutral collisions, as the mean-free path in this region is in the order of 1.5 μm [86]. The voltage at which ions are accelerated into the collision cell (mean free path 500 μm at 2 e^{-2} mbar [86]) can also be increased to 200 V and results in effective declustering. The pressure in this region is high enough that accelerating ions up to 200V does not impact their stopping distance. Collision cell modifications (Q-ToF Ultima [51]) have been described where the applied voltage was increased to 400 V [101]. When using the early Synapt G1 MS instrument [51], it was observed that improved high *m/z* transmission and protein complex delustering was achieved when the mobility gas (N_2) was present in the traveling wave ion mobility (TWIM [79]) cell and the TWIM trapping voltages were turned off (no mobility separation taking place). As opposed to the TWIM cell being evacuated and the MS being operated in MS mode only (personal observation). In the Orbitrap instrument, effective declustering occurs by "in source" CAD, immediately after the S-lens [102], or in the HCD cell [55] [103]. Effective ion activation and declustering has also been described for MDa complexes within both the C-Trap and the Orbitrap analyzer [104]. However, it is not clear if the radial path (up to 10 km depending on transient time [104]) of ions of lower *m/z* in the Orbitrap device contributes to any meaningful residual solvent removal. Finally, before the routine use of ion mobility for native-MS applications [60, 92, 93], the extent of gas-phase unfolding [105] was not fully appreciated when using higher source and collision cell voltages.

Time-of-Flight Optics: An ion's flight time (*t*) is proportional to the square root of its mass-to-charge ratio and is described by Equation 2, reproduced form reference [106]:

$$t = \frac{L}{v} = L\sqrt{\frac{m}{2qU}} \qquad (2)$$

Where *L* is the length of the drift space, *v* is the ion velocity, *m* is the mass of the ion (in kg) and *q* is the charge (where a single charge equates to 1.602×10^{-19} Coulomb) and *U* is the ion energy, in volts. If one considers the Waters Q-ToF instrument [66, 68, 94] the maximum upper ToF range was *m/z* 100,000, which equates to a flight time of 450 µsec and an instrument determined pusher frequency of 2.22 kHz [66] (Figure 5a). If one considers the early viral capsid work of Tito [54] (*m/z* values >20,000) and the GroEL tandem-MS experiments described by Lorenzen [94], in the latter example, there is an approximate 38,000 *m/z* span (monomer 57 kDa, *m/z* 2000-5000, to dodecamer 688 kDa *m/z* 30,000-40,000), therefore the pusher frequency must be set to the flight time of highest *m/z* value.

The associated analyzer resolution on isotopically resolved data (and not the peak width of an isotopically unresolved and adducted and/or solvated protein charge state) is relatively consistent across a very broad *m/z* range [19, 107, 108], as demonstrated by Sobott [66], where the instrument resolution was 10k FHWM at *m/z* 22,226 (Figure 6a) and is described by Equation 3, reproduced and modified from reference [106]:

$$R_{\Delta u} = \frac{m}{\Delta m} = \frac{u}{\Delta u} = \frac{t}{2\Delta t} \qquad (3)$$

where the resolution *R* (typically the FWHM definition; Equation 1, Supporting Information) is only determined by the energy spread (Δu), *t* is the ions flight time and Δt is its width, as a result of the special and velocity spread, in the field-free ToF region.

ToF analyzers are ideal detectors for high *m/z* species as the *m/z* range is theoretically unlimited [106]. However, there are practical limitations such as reduced MCP detection efficiency (~11%)

for large lower-speed ions [109]. This can be overcome by increasing the voltage gain on the MCP detector (personal observation).

The spatial volume of a ToF analyzer is large, therefore space charge effects is not a practical issue for a single pass reflectron based instrument. This is not the case for multi-reflective ToF MS instruments [110]. However, if ion counts are too high, time-to-digital (TDC) converter saturation does occur [111], therefore, limiting mass measurement accuracy. However, this is rarely ever realized when performing native-MS, as ion currents are generally low. From an Orbitrap perspective, charge capacity is carefully controlled on the Orbitrap MS instruments, using the automatic gain control function, which is typically set to 2 e^6 charges. In 2009, Waters described a new inhouse developed analogue to digital converter (ADC) detection system [112]. Ion saturation effects were significantly reduced, dynamic range increases realized, and still capable of exquisite high *m/z* detection [77].

The grids that make up specific regions in the oa-pusher and also the reflectron do have the ability to deflect the trajectory of the ions, therefore creating an additional source of peak broadening [108]. Sobott described a reduced gridline density from 1000 to 200 lines/inch for two regions within the oa-pusher stack [66] (Figure 5a). It was hypothesized that large proteins or protein/protein complexes with large cross sections may undergo unwanted scattering with the standard and higher line density grids.

Oa-ToF detectors typically operate at low e^{-6} to mid e^{-7} mbar pressures, compared to the higher vacuum of the Orbitrap and ICR instrument that are typically in the e^{-9} to e^{-10} mbar values, due to the ultralong ion paths and requirements to minimize ion-neutral collisions. As briefly mentioned earlier, when Xe was used as the collision gas on a Q-ToF, the ToF vacuum would reduce in efficiency to high e^{-6} mbar, due to Xe bleeding into the ToF analyzer and not being effectively evacuated. Reductions in ToF vacuum efficiencies were not observed when using SF_6 (personal observation). This observation may be related to polyatomic gases having consistently higher compression ratios (K_0) than monoatomic gases [113] in the pressure regimes that ToF operating in ($<e^{-4}$ mbar). However, it must be noted that the standard penning pressure gauge used on most MS systems is not universally calibrated for all gases, therefore likely show inconsistent pressure values across different gases.

Finally, calculated MW mass accuracies for native-MS (FT-ICR) measured versus denatured (reversed phased liquid chromatographic MS; oa-ToF) species (IgG1) are highly comparable [97].

Native-MS for All: A Dedicated Instrument for High m/z Analysis

As described in the aforementioned sections, the rapid progress in high *m/z* native-MS from the mid-90s through the late 2000s was routinely performed using oa-ToF analyzers and microchannel plate detection. Then, in 2012, there was a paradigm shift in native-MS data acquisition. Rose [55] published nESI native-MS spectra for a mAb, proteasome 20S complex and of course GroEL (including ATP bound), using a modified Orbitrap Exactive Plus, later commercially named as the Orbitrap Extended Mass Range (EMR). Briefly, it must be noted that Sharon [114] (in 2013) also presented well resolved ATP bound GroEL charge states, acquired on a Q-ToF instrument. In twelve years, the Orbitrap analyzer had undergone dramatic levels of refinement and optimization from that originally described by Makarov in 2000 [115]. Of note on this new Orbitrap EMR, are a source stacked ring ion guide (S-lens [116, 117]); a bent flatapole where collisional cooling occurs; an additional Xe gas line on the HCD cell; HCD voltages from 100 to 200 V applied to improved protein detection, transmission and desolvation (analogous to Q-ToF collision cell CAD experiments); increased *m/z* range of 400-24,000; Orbitrap detector pressures ranging from 5×10^{-10} and 2×10^{-9} mbar and the typical resolution setting was 17,500 at *m/z* 200. The fact that the Orbitrap could acquire both proteomics RPLC-MS/MS data [118] and now high *m/z* native-MS data, made this a highly disruptive and attractive technology.

Briefly, ion movement around the Orbitrap central electrode is complex, detection is image current based [115], followed by eFT [119] into frequency and therefore *m/z*. However, the true power of this new Orbitrap-based native-MS instrument was in the quality of the *m/z* spectral data. This was the first time that native charge states, high on the *m/z* scale (> *m/z* 5000) appeared to be fully desolvated, baseline resolved and close to their theoretical isotopic peak widths [55]. These MS spectral improvements were realized through the accurate knowledge of the initial phase of the ion packet entering the detector from the C-Trap, a level of real-time apodization, and a combination of magnitude mode [21] data at the base of mass spectral peak and absorption

mode [120] forming the top of the peak and an interpolation between these two extremes, forming the central portion of the peak [119, 121].

The Orbitrap continued to prove itself as more than a rival for oa-ToF detection and analysis of high MW species. Snijder [122] described the detection of an intact 4.5 MDa viral capsid with exquisite charge state definition at *m/z* 24,000. It must be noted that one year prior to this, Snijder [123] also reported a viral capsid of 18 MDa, displaying partially resolved charged states at *m/z* 50,000, reported from a modified Q-ToF2 instrument (*circa* 1999 [51]). Then in 2016, there was a direct comparison of oa-ToF and Orbitrap technology [124] for viral particle analysis and unsurprisingly, the Orbitrap charge state apparent resolution and levels of desolvation were superior (Figures 7a-d). Finally, preceding all the aforementioned work, in 2008 native-MS of the intact 3-4 MDa Hepatitis B virus particle was demonstrated by travelling wave ion mobility mass spectrometry [85, 125].

The next dedicated Orbitrap based instrument designed for high *m/z* transmission, selection and detection was the Orbitrap ultra-high mass range (UHMR [102]), that now possesses a quadrupole for high *m/z* precursor selection and additional ion activation capabilities. Belov [56] first described a precursor to the commercial UHMR (Figure 7e). Presented was exquisite pyruvate kinase isoform charge state definition, pyruvate kinase and GroEL tandem-MS and MS^3 generated fragment ion information. Of note, this model of Orbitrap used an RF-only dual ion funnel with orthogonal injection for the transfer capillary, where the first ion funnel operated at 12 mbar likely providing very effective collisional cooling. Collisional cooling also takes place in the bent flatapole region [56] (Figure 7e) likely by a similar method to that described by Thomson [67]. A quadrupole allowing for *m/z* 20,000 ion selection and an improved image current preamplifier with improved linearity and high-pass filter cutoff was also implemented. Three years later, Gault et al. also described a tandem-MS Orbitrap system for membrane protein analysis [103] using the UHMR. More recently, subtle effects of ion motion, such as eccentric and non-circular orbits have been documented, that may impact the radial distance and therefore the induced image current. Other small effects such as electronic noise of the pre-amplifier transistors that may be impacting charge assignment, have also be observed, although, only reported for MDa species [104].

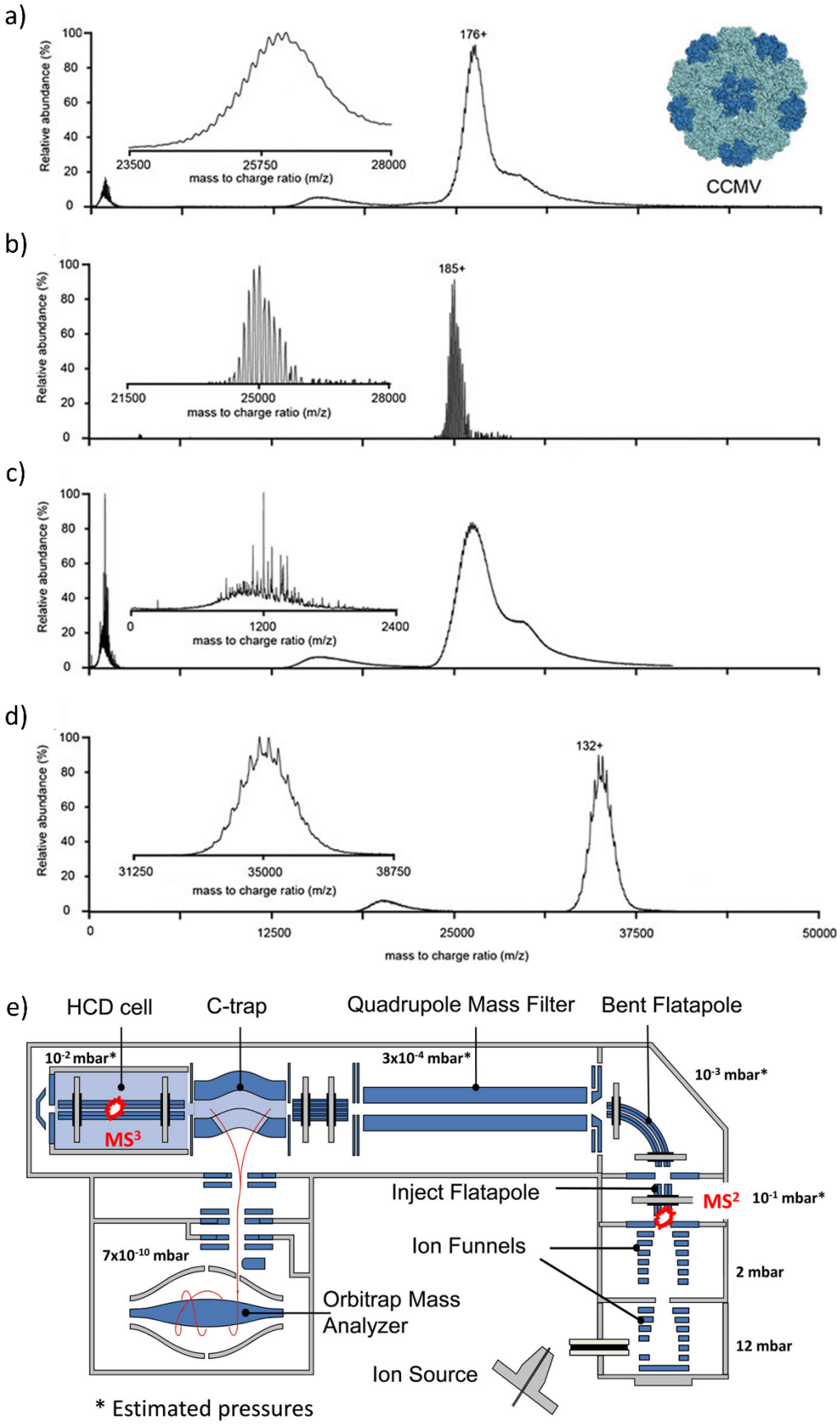
a)
Relative abundance (%)
100
80
60
40
20
0
176+
23500
25750
28000
mass to charge ratio (m/z)
CCMV
b)
Relative abundance (%)
185+
21500
25000
28000
mass to charge ratio (m/z)
c)
Relative abundance (%)
0
1200
2400
mass to charge ratio (m/z)
d)
Relative abundance (%)
132+
31250
35000
38750
mass to charge ratio (m/z)
0
12500
25000
37500
50000
mass to charge ratio (m/z)
e)
HCD cell
C-trap
Quadrupole Mass Filter
Bent Flatapole
10-2 mbar*
3x10-4 mbar*
10-3 mbar*
MS3
Inject Flatapole
MS2
10-1 mbar*
Ion Funnels
7x10-10 mbar
2 mbar
Orbitrap Mass Analyzer
12 mbar
Ion Source
* Estimated pressures

Figure 7. Native mass spectra of multipartite CCMV endogenous virions acquired under different experimental conditions using different mass spectrometer. a) Spectrum acquired using a Q-ToF. A single series of resolved charge states can be resolved at high collisional activation; b) Spectrum acquired on an Orbitrap EMR with extended mass range, displaying baseline resolved ion signals; c) All ion fragmentation of CCMV on the quadrupole time-of-flight instrument; d) Q-ToF spectrum after charge reduction using triethylammonium acetate. Reproduced from reference [124], with permission from the American Chemical Society, Copyright 2016; e) Schematic diagram of the modified Orbitrap Q-Exactive mass spectrometer. Reproduced from reference [56], with permission from the American Chemical Society, Copyright 2013.

Regular "Off-the-Shelf" MS Instruments are Still Good Enough

It must be noted that other commercial, non-bespoke MS instruments still remain an option for high *m/z* transmission and detection, and therefore native-MS studies. If we consider the FT-ICR MS instrument and the following Equation 4 [21, 126]:

$$m_{critical} = \frac{1.20607\text{x}10^{7} z B_0^2 a^2}{V_{trap}\alpha} \qquad (4)$$

where M_{critical} is in Da, B is magnetic field strength in Tesla, V_{trap} is in volts, z in multiples of elementary charge, α is a dimension referring to the length of the Infinity cell, in meters [21].

Throughout FT-ICR evolution, arguably it never appeared that this MS instrument was being focused for high *m/z* analysis, but rather smaller ionic species, such as petroleomics [127] and ultrahigh resolution analytics [128]. As Li [126] notes, the current 15 Tesla FT-ICR is more than capable of trapping species of 1 MDa. Additionally, the majority of the recent high *m/z* FT-ICR research, outline below, utilized the Infinity cell [129]. For example, Li [126] demonstrated aggregated β-galactosidase and charged reduced glycogen phosphorylase at *m/z* values 17,000 and 25,000, respectively. Campuzano[86, 130 57] demonstrated just how flexible the 15 Tesla FT-ICR MS is for native-MS analysis for a very broad range of analytes (CsI clusters, mAbs, ADCs, nanodiscs,

membrane proteins and large multiunit complexes; Figure 4). Cytochrome P3A4 hexamer ejection from a loaded nanodisc was demonstrated, producing well resolved charged states at *m/z* 7000-9000, equating to a intact hexameric MW of 308 kDa [131] (Figure S2, Supporting Information). Finally, the 1.61 MDa GroEL dimer, with *m/z* values of 14,000-15,500 has also been demonstrated [57].

The current native-MS data that is being generated on the FT-ICR is also comparable to that of the Orbitrap [55, 56, 103, 132], when the FT-ICR data is either acquired directly in absorption mode (aFT; for mAbs [133]) or post-acquisition aFT processed, recently described for nanodiscs [87]. MAb native-MS aFT acquired data is displayed in Figure 8a. The FT-ICR MS footprint has also significantly reduced. For example, the latest iteration, the scimaX [134] (7 Tesla conduction cooled magnet; Bruker Daltonics) is more than capable of detecting GroEL, with zero instrument optimization [57] .

Finally, a highly relevant but rarely referenced piece of work, is that by Heck and van den Heuvel from two decades ago [63]. They demonstrated measured charge states at *m/z* values 10,000 to 12,000 for the octameric vanillyl-alcohol oxidase, using an LCQ-Deca ion trap mass spectrometer.

Subtle and Applied Ion Source Design Considerations

In 2011 Waters introduced the StepWave [135, 136] ion guide, which did not require pressure modifications for high *m/z* transmission. This ion source was a significant change from the original hexapole ion guide of the early Q-ToF instruments [50, 51], and somewhat similar to the dual series oriented stacked ring ion guides [79] of the Q-ToF Ultima (*circa* 2000 [51]) and the later generation single stacked ring ion guide of the Q-ToF Premier (*circa* 2003 [51]). The StepWave source operates at a much higher gas flow than earlier generation sources and therefore higher pressures. It is estimated the pressure in the first StepWave ion guide is approximately 3 mbar. Therefore, the area immediately preceding the first ion guide (source backing region) will be significantly higher, likely affording highly effective collisional cooling. As a result, high *m/z* transmission is efficient on the StepWave enabled MS instrument. Giles [135] and Harrison [137] described effective transmission and subsequent detection of GroEL (802 kDa) and urease (545

kDa) respectively, on a StepWave enabled Q-ToF MS. Recent StepWave ion guide developments utilize RF enhanced ion declustering in the second SRIG [138]. Churneschevich [67] noted the SCIEX QqToF MS prototype with the inline source configuration did not require elevated interface pressure for optimized high *m/z* transmission.

The Orbitrap EMR [55] (S-lens), the precursor to the UHMR [56] (dual ion funnel), the commercial UHMR [139] (S-lens), the next generation tribrids, the LUMOS [140] and the Eclipse [141] (both single funnel) and FT-ICR MS [57] (dual funnel) instruments have all shown impressive high *m/z* transmission capabilities. The source S-lens or funnels, operate at similar or higher pressures than those reported on the original Micromass/Waters LCT [51, 73] and Q-ToF [50, 51] instrument. For example, the standard UHMR Orbitrap S-lens operates at ~1.4-1.8 mbar (software derived; XCalibur). The first (of two) funnels described by Belov [56] (Figure 7e) operates at 12 mbar with orthogonal injection. Therefore, in both, cases it can be inferred that the ion transfer capillaries operate at higher pressures, therefore providing sufficient collisional cooling, therefore source pressure adjustment is not required. The same inferences can be made for the heated capillary preceding the dual ion funnel source, with orthogonal ion sampling configuration of the solariX ion optics cart [57]. It must be noted that Krutchinksy [43] utilized a heated metal transfer capillary for improved protein complex desolvation.

The commercial UHMR implemented in-source trapping (between the S-lens exit and the flatapole entrance) dramatically improving high *m/z* desolvation [102]

There is precedent to investigate the perceived superior desolvation capabilities of the S-lens on a non-Orbitrap MS platform. Close to a decade ago, an inline heated capillary S-lens source was hyphenated to a Micromass Q-ToF 2 [142]. The findings suggest the S-lens (operated at 6 mbar) had little effect on mAb desolvation. The critical area was still the hexapole transfer lens and its optimized pressure (~2 e^{-2} mbar). This observation may also suggest the benefits that eFT [119] (and absorption mode FT processing; Figure 8a) data processing affords for Orbitrap spectral data quality for native-MS applications. It must be noted that the lens spacing in the Waters based SRIGs described by Giles [79] are equivalent (center to center spacing of 1.5 mm). As opposed to increase center-to-center spacing of the S-lens (1 mm to 5 mm [143]) which increases the confining RF field as the ion cloud travel through the device [117].

One important point of note is that both aforementioned Orbitrap and Bruker source designs use mostly in-line nESI sample introduction (Supporting information, Figures S3a & b, Supporting Information). This is not the case for the original Z-spray source (Figure S3c; off axis, dual orthogonal sampling). Additionally, the Bruker solariX source utilizes a partial vacuum orthogonal sampling stage as the ions exit the heated transfer capillary prior to ion funnel entry (Figure S4, Supporting information). Never-the-less, all current MS source designs, with or without modifications and/or pressure optimizations, appear to operate well for high *m/z* transmission.

An important consideration is the temperature at which the ions are introduced into the MS source. For example, native-MS nESI experiments performed on the Bruker 15 Tesla FT-ICR and Orbitrap EMR, the transfer capillaries have been documented to operate over a broad range of temperatures (40 °C to 200 °C [86, 103, 130]). Large and measurable differences in ion solvation/adducting have been observed on the solariX source if operated at ambient versus elevated temperatures [57]. Native-MS nESI experiments using the Waters Z-Spray source are mostly acquired at ambient temperatures [64].

Is the Term High Resolution Native-MS Accurate or Appropriate?

The term "high-resolution" for native-MS [100, 103, 144] and general protein MS [145] has coincided with the Orbitraps superior native and denatured-MS spectral quality, therefore must be addressed in the context of this MS instrument evolution discussion. The question is, do the new MS instruments afford true high resolution native-MS data? and is this new term linked to the *m/z* peak resolution (Equation 1, Supporting Information) [146] or the instrument measured resolving power (Equation 2, Supporting Information) [146], , or another MS property?

Described earlier (Equation 3) oa-ToF MS resolution is relatively consistent across a very broad *m/z* range [19, 107, 108]. This is in stark contrast to that of the Orbitrap where the MS resolution, *R* (or more commonly defined as resolving power in ICR MS instrumentation, Equation 2, Supporting Information) decreases as a square root of *m/z* [147, 148 149], as descried by Equation 5:

$$R = \frac{m}{\Delta m_{50\%}} = -\frac{1}{2\Delta\omega_{50\%}}\sqrt{\frac{kq}{m}} \qquad (5)$$

Where $\boldsymbol{\omega}$ is the axial oscillations (frequency), q is the electronic charge of an electron in Coulombs ($1.602e^{-19}$) and k is field curvature value. In contrast to the ICR frequency which varies inversely with the *m/z* [21, 148] descried by Equation 6, reproduced from Marshall [21]:

$$R = \frac{m}{\Delta m_{50\%}} = -\frac{qB_0}{m\Delta\omega_{50\%}} \qquad (6)$$

which in practical terms means, as the *m/z* doubles, the resolution reduces by approximately 1.41 and two-fold on the Orbitrap and FT-ICR MS instrument, respectively (Table S1, Figures S5a & S5b, Supporting Information). Therefore, representative oa-ToF native and denatured MS acquisitions, where the MS instrument resolution (Equation 2, Supporting Information) is typically 10k-14k FWHM [6, 97, 150, 151] is in fact comparable, or even higher to those used on the Orbitraps instruments over similar *m/z* ranges [55, 56, 86, 103, 132, 145]. Therefore, the aforementioned Orbitrap native and denatured-MS data is far from high resolution if one considers the MS instrument resolution at which the data was acquired.

In 1998 Shi [128] demonstrated fine isotopic structure of insulin, using a 9.4 T FT-ICR instrument using a 3 s transient, which equates to an instrument resolving power of 5 M at *m/z* 300. If one extends this description of resolving power to larger proteins, specifically those acquired by Orbitrap MS, then one can consider the first isotopically resolved mAb data by Shaw [152] (3 s transient length, resolving power 330 k at *m/z* 2800; Figure 8b) as high resolution protein data. Mass accuracies are compared (3.1 vs 5.0 ppm) to lower resolving power oaToF MS instrument acquisitions [97, 153]. McGee et al. [154], using Orbitrap-based single ion counting, presented high-resolution native-MS whereby isotopically resolved protein complexes (Figure 8c), up to MW 466 kDa, were achieved.

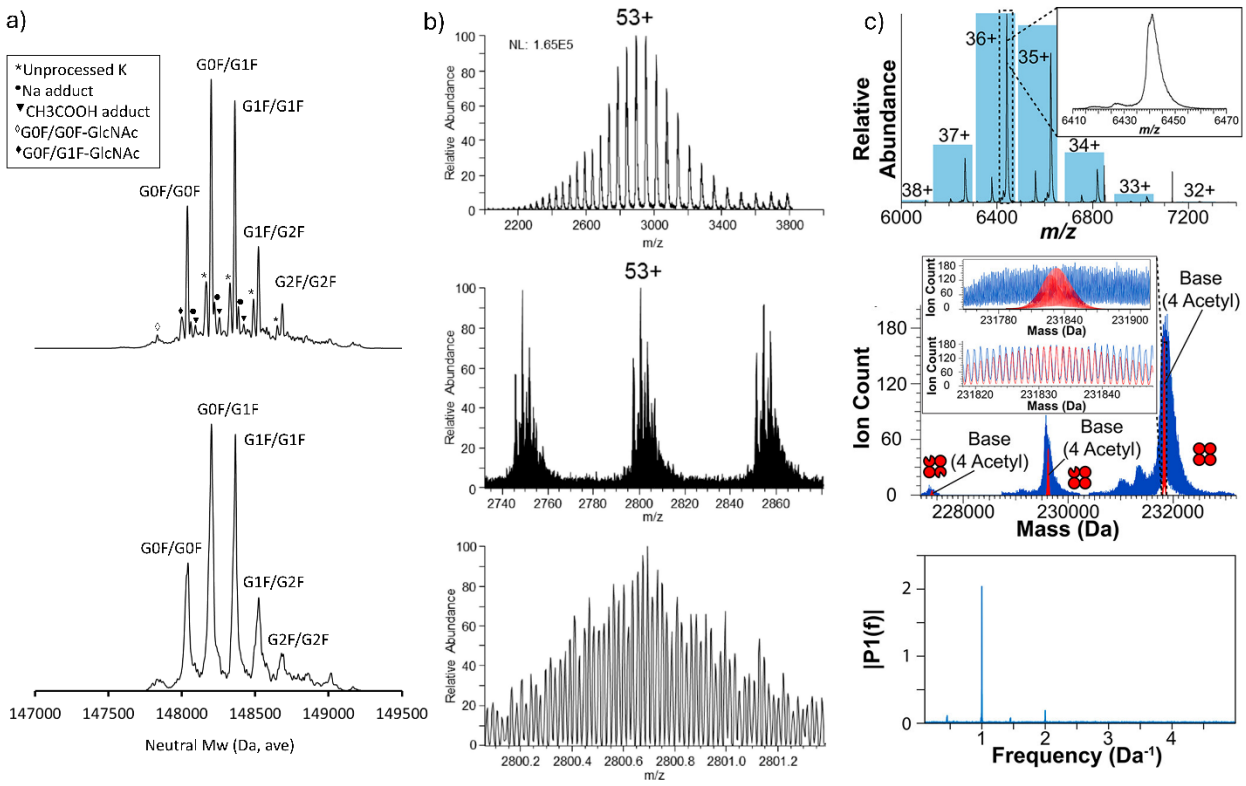

Figure 8. A selection of high-resolution protein data acquired by FT-ICR and Orbitrap MS; a) native-MS deconvolved spectrum of the NIST IgG1*k* mAb acquired by nESI (1 minute acquisition; 5 uM, in 200 mM ammonium acetate, skimmer 25 V, collision cell 30 V) using a solariX 15 Tesla FT-ICR MS system using a transient size and length of 1 M and 0.68 sec, respectively. The data was acquired directly in absorption mode using the FTMS Booster X3 (Spectroswiss). Both magnitude (lower spectrum) and absorption (upper spectrum) mode data were acquired, displayed and processed using the Spectroswiss PeakbyPeak FTMS data analysis software (v2021.8.0). The transient was apodized using a semi-Kaiser function with zero transient truncation. Deconvolution was performed using Protein Metrics Intact [97, 155]. The main glycoforms are annotated and minor truncated species are tabulated; b) a mAb acquired in the ion trap (upper); three selected charge states acquired by Orbitrap FT-MS (middle) and a zoomed-in regions for the $z = 53^+$ charge state showing fine isotopic structures. Reproduced and modified from reference [152] with permission from the American Chemical Society, Copyright 2013 and c) a native mass spectrum of pyruvate kinase in the *m*/*z* domain created by averaging 26339 unprocessed spectra. The inset shows an expansion of the most abundant charge state. The histogram overlay shows the relative abundance of ions assigned to charge states via the I^{2}MS

workflow (upper). The experimental I^2MS mass spectrum of pyruvate kinase (blue trace) overlaid with the theoretical isotopic distribution calculated for a tetramer of pyruvate kinase where the base sequence of each monomer was modified with N-terminal acetylation (red trace). The secondary and tertiary distributions of pyruvate kinase correspond to tetrameric complexes that have one and two N-terminally truncated monomers, respectively (middle). Data obtained by Fourier transformation of the mass distribution of pyruvate kinase from panel b (lower figure). Reproduced and modified from reference [154] with permission from the American Chemical Society, Copyright 2021.

There is an additional line of discussion which must be considered in the context of the term high resolution native-MS. It is tempting to describe Orbitrap native-MS charge states, and mAb glycoforms [55, 132] and GroEL for example, that are well separated from each other, baseline resolved and appear to be of theoretical isotopic peak width [55] as high resolution native-MS data. All of which are still somewhat challenging to achieve on an oa-ToF instrument [97, 151, 156] (progress is being made by using post-acquisition processing to improve oa-ToF data quality, such as inverse FT and apodization [157]). A descriptive term, and one in which we are more aligned, and we believe more accurately describes the aforementioned protein data quality (especially native-MS data) and have previously introduced, in 2020, as "highly desolvated" ions [57]. Groups have also described the strong and improved desolvation and ion cooling capabilities of the Orbitrap instrument [86, 103, 139, 158]. Narrower, more desolvated charge states were recently described for CD-MS by Worner [104].

Therefore, the term high resolution native-MS may not be an appropriate description for ionic species that may have been effectively desolvated, and data captured that is a function of enhanced FT (eFT) acquisition [119, 121]. Therefore, how should one describe this new paradigm shift in native-MS data quality which is not isotopically resolved, possibly still adducted and acquired at low instrument resolving power? We are suggesting the term "resolved native-MS data".

Future Instrument Developments

Native-MS and high *m/z* analysis has become much more routine, useable and accessible due to the development of ESI [13] [14] enabling generation of gas-phase native-like biological ions, subsequent detection and exquisite characterization by the MS technologies described herein. MS instrumentation also offers multiple fragmentation techniques [88] [159] [160] [161] [162] [141, 163] [164] [165] [166]. We argue that for high *m/z* and native-MS analyses, all of the above fragmentation methods and ion mobility capabilities such as drift tube [93, 167], travelling wave [60, 77, 79, 168] and trapped ion mobility [169] [170], have been enabled by ESI, and benefitted from the source and detector modifications described above, therefore will not be described further.

Over the past decade charge reduction has been used to effectively generate ions that possess low levels of overall charge. For example Lermyte [171] described how glow discharge based electron transfer dissociation effectively charge reduces pyruvate kinase in the MS source of a Q-ToF, to a $z = 2^+$ ion, with an *m/z* value of 117,000. Over a decade later, the same group demonstrated extensive levels of charge reduction including a GroEL $z = 7^+$ ion and AAV8 charge reduced ions up to *m/z* 200,000, using the Orbitrap analyzer [172]. One of the most impressive and recent demonstrations of charge reduction is the work of Bhanot [173] where a $z = 2^+$ GroEL charge state (*m/z* 400,000) was generated, transmitted and detected on a relatively unmodified Triple ToF 5600 (SCIEX). Moreover, the authors discuss how the ion cloud size increases as the overall charge (z) decreases, thus impacting ion transmission and detection efficiency. Much of this work is based on the seminal ion/ion chemistry work originally described by McLuckey [174]. Additionally, routine charge reduction and therefore high *m/z* formation was made somewhat routine on the Orbitrap MS through commercialization of the Proton Transfer Charge Reduction [175], much like glow discharge on the Q-ToF MS [176]. Preceding many of the aforementioned examples, Campuzano and Schnier [177], using corona discharge based on the original designs of Smith [178] (in earlier iterations of charge reduction, Smith also used ^{210}Po [179]) demonstrated effective charge reduction and high *m/z* transmission for PEG and multi-subunit protein complexes, including GroEL. Nevertheless, all these described studies were performed on mostly standard MS platforms, demonstrating the inherent high *m/z* capabilities of these instruments, and the potential of charge reduction, in its various forms. The recent development of digital ion traps and quadrupoles has proven their worth for both high *m/z* transmission (β-galactosidase, *m/z* 30,000 [180]; ribosome 70S, *m/z* 100,000 to 110,000 [181]) and selection (GroEL; *m/z* 13,000, $z = 62^+$ isolation [182]) respectively, by manipulating the waveform frequency.

A technology now being successfully used for ultra-high mass detection is charge detection, which is particularly enabling for MW measurement of highly polydisperse species, is charge detection mass spectrometry (CD-MS). Originally described in the mid-1990s by Benner [183] and further developed by Jarrold [184] and Williams [185] evolving in to technologies capable of ultrahigh MW measurements. For example, Jarrold has recorded adenovirus species of 63 MDa and 134 MDa [186] and Williams has recently recorded nanodrop sizes of 40 nm to 120 nm with recorded MWs of 50 MDa to 550 MDa [187].

A commercial version of CD-MS was showcased by Heck (IgM complex, >1MDa [188]) and Kafader [189] describing single-particle charge detection on an Orbitrap MS. Another exciting hyphenation of technologies, is the recent combination of the single particle counting based nanoelectromechanical system (NEMS) to both ToF [190] and Orbitrap [191] mass spectrometer instrument. Where the authors have demonstrated a MW measurements ranging from kDa to MDa (IgMs and gold nanoparticles [192]) to the well-known native-MS standard, that is GroEL [191].

A potential emerging highly enabling technology for gas-phase structural biology is soft-landing. Originally described Volny [193] and later by Cooks [194], then first documented for native-MS analysis of aqueous soluble protein complexes, by Mikhailov [195] on a QToF instrument. Recently soft landing has been implemented on the Orbitrap instrument [196]. The ability to *m/z*-select large, protein ions, even from complex mixtures, and land them onto a grid for cryogenic electron microscopy (cryoEM) could potentially advance structural biology studies of large protein complexes. The aforementioned soft-landing methods benefit from the high *m/z*, high MW transmission capabilities of the MS instruments to which EM is hyphenated to [190, 191]. Prefacing the above MS-EM example, MS has historically been described to support both X-ray crystallography and NMR high resolution structure determination [197].

From a native-MS sample introduction perspective, two methods can be considered. The first being the nESI singe shot glass vial [49 48] where the user can exquisitely control the flow rate and levels of desolvation, but throughput for this method is clearly low. The Advion nanomate [198] can add the required level of automation and throughput to the aforementioned nESI method. The second method, that is much higher throughput, automated and platformable, is direct chromatographic hyphenation to the MS. This is achieved by using ammonium acetate mobile phases for SEC [199], CEX [200] and HIC [201]. Recently online detergent exchange was demonstrated

for membrane protein complexes [202] SEC has also been hyphenated to charge detection MS [203]. Finally, this level of hyphenation and automation is essential within the biopharmaceutical setting where sample numbers are high [6].

Concluding Remarks

Herein we have described the early pioneering high *m/z* CsI FT-ICR MS data acquisitions and then the first ever native-MS acquisitions in the form of myoglobin and ADH. We then discussed the first and essential Q-ToF bespoke modifications (source, quadrupole, collision cell and associated gases and oaToF pusher frequency modifications) that enabled the gentle transfer of proteins and protein complexes into the gas phase of the MS, and their detection. We discussed the concept of axial and radial ion collisional cooling and its critical importance to high *m/z* preservation, transmission and detection. We then discussed the newer generation of Orbitrap-based MS instrumentation specifically focused on high *m/z* transmission, detection and importantly the dramatically improved native-MS spectral data quality. Also discussed is how current and standard MS instrumentation are more than capable of retaining non-covalent complexes, transmitting, detecting these high *m/z* ions in the gas-phase of the MS. In the future instrumental section, we discuss recent ultra-high *m/z* detection on traditional MS platforms (ao-ToF and Orbitrap) but also consider newer charge detection-based instruments. We also highlight sample introduction improvements and the clear need for native chromatographic hyphenation that will enable a more "platformed" approaches to native-MS.

Over the past two decades there has been a clear realization from MS instrument manufacturers that high *m/z* transmission and detection by MS users is an important field for both research and applied applications. Therefore, MS instrumentation has evolved from bespoke modifications through to higher volume specific instruments, that are capable of both small and large ion analytics.

What was perceived as an art-form some two and a half decades ago, high *m/z* generation, transmission, detection (native-MS) has become far more attainable to more scientists, in more laboratories across a more diverse range of functions, because of the aforementioned instrument and sample introduction developments and associated methods.

Finally, let us not forget about negative ion polarity. Groups have demonstrated that negative ion mode nESI is more that capable of producing useable native-MS spectra, recording ions higher in the *m/z* range than the equivalent positive ion mode spectra for multimeric protein complexes [204]. For example, the negative ion nESI GroEL displays well resolved charge states at *m/z* 14,000 [97] (Figure S6, Supporting Information) and the negative ion nESI of CsI displays measured ions above *m/z* 18,000 [97] (Figure S7, Supporting Information).

Acknowledgements

The authors would like to thank Kevin Giles, Jeff Brown and Martin Palmer (Waters Corporation. MS Technologies Center, Manchester, UK) for the useful discussions regarding high mass quadrupoles, StepWave ion source optics and pressures. The authors also wish to thank Rachel Ogorzalek Loo (UCLA) and Elizabeth Duselis (AbbVie) for the useful discussions regards instrument vacuum systems and collisional cooling considerations. We also wish to thank Mike W. Senko and Julian Saba (Thermo Scientific, San Jose, USA) for the useful discussions regards Orbitrap source S-lenses, ion funnels and associated references. We also wish to thank Jan Commandeur (MS Vision) for being so willing to share unpublished data that describes the hyphenation of an S-lens source to a Q-ToF MS. Finally, we also wish to thank Elizabeth Hecht (Amgen) for critically proof-reading this article. The GroEL PDB file 4V43 displayed in the graphical abstract, was downloaded from www.rcsb.org. The authors also wish to acknowledge that the abstract for this article was refined using Microsoft Copilot. J.A.L. acknowledges support from the US National Institutes of Health (R35GM145286) and the US Department of Energy (DE-FC02-02ER63421). The authors declare no Conflict of Interest.

Supporting Information

Additional and Personal Observations for: Noncovalent Complexes become Larger and *m/z* Values Higher; What is High *m/z* Now? Ion Declustering and Time-of-Flight Optics; A quadrupole RF-transmission profile plot; NanoESI analysis of the CYP3A4 loaded nanodisc on a solariX 15 Tesla FT-ICR MS; Bruker, Thermo Scientific and Waters Z-Spray sources; the solariX 15 Tesla FT-ICR schematics; Is the Term High Resolution Native-MS Accurate or

Appropriate; Future Instrument Developments? A theoretical resolution comparison between the Orbitrap UHMR and the solariX 15 Tesla FT-ICR MS instruments; Comparisons of CsI acquired on the solariX 15 Tesla FT-ICR and the Orbitrap UHMR.; Negative ion mode nESI of GroEL; Positive versus negative ion mode nESI comparison of CsI.

References

(1) Pellecchia, M.; Sem, D. S.; Wuthrich, K. NMR in drug discovery. *Nat Rev Drug Discov* **2002**, *1* (3), 211-219. DOI: 10.1038/nrd748.
(2) Olaru, A.; Bala, C.; Jaffrezic-Renault, N.; Aboul-Enein, H. Y. Surface plasmon resonance (SPR) biosensors in pharmaceutical analysis. *Crit Rev Anal Chem* **2015**, *45* (2), 97-105. DOI: 10.1080/10408347.2014.881250.
(3) Hong, P.; Koza, S.; Bouvier, E. S. Size-Exclusion Chromatography for the Analysis of Protein Biotherapeutics and their Aggregates. *J Liq Chromatogr Relat Technol* **2012**, *35* (20), 2923-2950. DOI: 10.1080/10826076.2012.743724. Haverick, M.; Mengisen, S.; Shameem, M.; Ambrogelly, A. Separation of mAbs molecular variants by analytical hydrophobic interaction chromatography HPLC: overview and applications. *MAbs* **2014**, *6* (4), 852-858. DOI: 10.4161/mabs.28693. Harris, R. J.; Kabakoff, B.; Macchi, F. D.; Shen, F. J.; Kwong, M.; Andya, J. D.; Shire, S. J.; Bjork, N.; Totpal, K.; Chen, A. B. Identification of multiple sources of charge heterogeneity in a recombinant antibody. *J Chromatogr B Biomed Sci Appl* **2001**, *752* (2), 233-245. DOI: 10.1016/s0378-4347(00)00548-x.
(4) Gillespie, T. A.; Winger, B. E. Mass spectrometry for small molecule pharmaceutical product development: a review. *Mass Spectrom Rev* **2011**, *30* (3), 479-490. DOI: 10.1002/mas.20289.
(5) Beck, A.; Wagner-Rousset, E.; Ayoub, D.; Van Dorsselaer, A.; Sanglier-Cianferani, S. Characterization of therapeutic antibodies and related products. *Anal Chem* **2013**, *85* (2), 715-736. DOI: 10.1021/ac3032355.
(6) Campuzano, I. D. G.; Sandoval, W. Denaturing and Native Mass Spectrometric Analytics for Biotherapeutic Drug Discovery Research: Historical, Current, and Future Personal Perspectives. *J Am Soc Mass Spectrom* **2021**, *32* (8), 1861-1885. DOI: 10.1021/jasms.1c00036.
(7) Campuzano, I. D. G.; Sandoval, W. Editorial: Special JASMS Focus on Mass Spectrometry in Industry. *J Am Soc Mass Spectrom* **2021**, *32* (8), 1850-1851. DOI: 10.1021/jasms.1c00214.
(8) Apostol, I.; Bondarenko, P. V.; Ren, D.; Semin, D. J.; Wu, C. H.; Zhang, Z.; Goudar, C. T. Enabling development, manufacturing, and regulatory approval of biotherapeutics through advances in mass spectrometry. *Curr Opin Biotechnol* **2021**, *71*, 206-215. DOI: 10.1016/j.copbio.2021.08.001 From NLM Medline.
(9) Khalikova, M.; Jires, J.; Horacek, O.; Dousa, M.; Kucera, R.; Novakova, L. What is the role of current mass spectrometry in pharmaceutical analysis? *Mass Spectrom Rev* **2024**, *43* (3), 560-609. DOI: 10.1002/mas.21858 From NLM Medline.
(10) Ivleva, V. B.; Schneck, N. A.; Gollapudi, D.; Arnold, F.; Cooper, J. W.; Lei, Q. P. Investigation of Sequence Clipping and Structural Heterogeneity of an HIV Broadly Neutralizing Antibody by a Comprehensive LC-MS Analysis. *J Am Soc Mass Spectrom* **2018**, *29* (7), 1512-1523. DOI: 10.1007/s13361-018-1968-0. Wallace, W. E.; Moorthy, A. S. NIST Mass Spectrometry Data Center standard reference libraries and software tools: Application to seized drug analysis. *J Forensic Sci* **2023**, *68* (5), 1484-1493. DOI: 10.1111/1556-4029.15284 From NLM Medline.

(11) Griffiths, J. A brief history of mass spectrometry. *Anal Chem* **2008**, *80* (15), 5678-5683. DOI: 10.1021/ac8013065 From NLM PubMed-not-MEDLINE. McLafferty, F. W. A century of progress in molecular mass spectrometry. *Annu Rev Anal Chem (Palo Alto Calif)* **2011**, *4*, 1-22. DOI: 10.1146/annurev-anchem-061010-114018 From NLM Medline.
(12) Karas, M.; Bachman, D.; Hillenkamp, F. Matrix-assisted ultraviolet laser desorption of non-volatile compounds. *Internation Journal of Mass Spectrometry Ion Processes* **1987**, *78*, 53-68. DOI: https://doi.org/10.1016/0168-1176(87)87041-6. Karas, M.; Hillenkamp, F. Laser desorption ionization of proteins with molecular masses exceeding 10,000 daltons. *Anal Chem* **1988**, *60* (20), 2299-2301. DOI: 10.1021/ac00171a028. Tanaka, K.; Waki, H.; Ido, Y.; Akita, S.; Yoshida, Y.; Yoshida, T. Protein and Polymer Analyses up to m/z 100,000 by Laser Ionization Time-of-flight Mass Spectrometry *Rapid Commun Mass Spectrom* **1988**, *2* (8), 151-153. Tanaka, K. The Origin of Macromolecule Ionization by Laser Irradiation. **https://www.nobelprize.org/prizes/chemistry/2002/tanaka/lecture/**.
(13) Yamashita, M.; Fenn, J. B. Electrospray ion source. Another variation on the free-jet theme. *J Phys Chem* **1984**, *88* (20), 4451-4459.
(14) Yamashita, M.; Fenn, J. B. Negative Ion Production with the Electrospray Ion Source. *Journal of Physical Chemistry* **1984**, *88*, 4671-4675. Fenn, J. B. Electrospray Wings for Molecular Elephants. **https://www.nobelprize.org/prizes/chemistry/2002/fenn/lecture/**.
(15) Verenchikov, A. N.; Krasnov, N. V.; Shkurov, V. A. Electrospray ionization developed by Lidija Gall's group. *International Journal of Mass Spectrometry* **2023**, *490*, 11067. DOI: https://doi.org/10.1016/j.ijms.2023.117067.
(16) Wilschefski, S. C.; Baxter, M. R. Inductively Coupled Plasma Mass Spectrometry: Introduction to Analytical Aspects. *Clin Biochem Rev* **2019**, *40* (3), 115-133. DOI: 10.33176/AACB-19-00024.
(17) Mann, M. Origins of mass spectrometry-based proteomics. *Nat Rev Mol Cell Biol* **2016**, *17* (11), 678. DOI: 10.1038/nrm.2016.135 From NLM Medline.
(18) Dawson, P. H. Quadrupole Mass Spectrometry and its Applications, 1st ed. American Institute of Physics: Woodbury, New York, 1995.
(19) Standing, K. G.; Vestal, M. L. Time-of-flight mass spectrometry (TOFMS): From niche to mainstream. *International Journal of Mass Spectrometry* **2015**, *377* (1 February), 295-308. DOI: https://doi.org/10.1016/j.ijms.2014.09.002.
(20) Coles, J.; Guilhaus, M. Orthogonal acceleration - a new direction for time-of-flight mass spectrometry: fast, sensitive mass analysis for continuous ion sources *Trends in Analytical Chemistry* **1993**, *12* (5), 203-213. DOI: https://doi.org/10.1016/0165-9936(93)80021-B.
(21) Marshall, A. G.; Hendrickson, C. L.; Jackson, G. S. Fourier transform ion cyclotron resonance mass spectrometry: a primer. *Mass Spectrom Rev* **1998**, *17* (1), 1-35. DOI: 10.1002/(SICI)1098-2787(1998)17:1<1::AID-MAS1>3.0.CO;2-K.
(22) van den Heuvel, R. H.; Heck, A. J. Native protein mass spectrometry: from intact oligomers to functional machineries. *Curr Opin Chem Biol* **2004**, *8* (5), 519-526. DOI: 10.1016/j.cbpa.2004.08.006.
(23) Marcoux, J.; Robinson, C. V. Twenty years of gas phase structural biology. *Structure* **2013**, *21* (9), 1541-1550. DOI: 10.1016/j.str.2013.08.002.
(24) Loo, J. A. Studying noncovalent protein complexes by electrospray ionisation mass spectrometry. *Mass Spectrometry Reviews* **1997**, *16*, 1-23.
(25) Benesch, J. L.; Ruotolo, B. T.; Simmons, D. A.; Robinson, C. V. Protein complexes in the gas phase: technology for structural genomics and proteomics. *Chem Rev* **2007**, *107* (8), 3544-3567. DOI: 10.1021/cr068289b.
(26) Benesch, J. L.; Ruotolo, B. T. Mass spectrometry: come of age for structural and dynamical biology. *Curr Opin Struct Biol* **2011**, *21* (5), 641-649. DOI: 10.1016/j.sbi.2011.08.002.

(27) Hilton, G. R.; Benesch, J. L. Two decades of studying non-covalent biomolecular assemblies by means of electrospray ionization mass spectrometry. *J R Soc Interface* **2012**, *9* (70), 801-816. DOI: 10.1098/rsif.2011.0823.
(28) Olinares, P. D. B.; Kang, J. Y.; Llewellyn, E.; Chiu, C.; Chen, J.; Malone, B.; Saecker, R. M.; Campbell, E. A.; Darst, S. A.; Chait, B. T. Native Mass Spectrometry-Based Screening for Optimal Sample Preparation in Single-Particle Cryo-EM. *Structure* **2021**, *29* (2), 186-195 e186. DOI: 10.1016/j.str.2020.11.001 From NLM Medline.
(29) Amster, J. I.; McLafferty, F. W.; Castro, M. E.; Russell, D. H.; Cody, R. B.; Ghaderi, S. Detection of Mass 16 241 Ions by Fourier-Transform Mass Spectrometry. *Analytical Chemistry* **1986**, *58*, 483-485.
(30) Lebrilla, C. B.; Wang, D. T.; Hunter, R. L.; McIver, R. T., Jr. Detection of mass 31,830 ions with an external ion source Fourier transform mass spectrometer. *Anal Chem* **1990**, *62* (8), 878-880.
(31) Amster, I. J.; Loo, J. A.; Furlong, J. J.; McLafferty, F. W. Cesium ion desorption ionization with Fourier transform mass spectrometry. *Anal Chem* **1987**, *59* (2), 313-317. DOI: 10.1021/ac00129a020 From NLM Medline.
(32) Kaiser, R. E., Jr.; Cooks, R. G.; Stafford, G. C.; Syka, J. E. P.; Hemberger, P. H. Operation of a Quadrupole Ion Trap Mass Spectrometer to Acheive High Mass/Charge Ratios. *International Journal of Mass Spectrometry and Ion Processes* **1991**, *106*, 79-115. DOI: https://doi.org/10.1016/0168-1176(91)85013-C.
(33) Morris, M.; Bateman, R.; Nicolaysen, L.; Brooks, V. The History of Magnetic Sector Mass Spectrometry at VG - Micromass - Waters. *https://www.asms.org/docs/default-source/history-posters/vendor_vg-sectors_36x18.pdf?sfvrsn=e63576c3_0*.
(34) Barber, M.; Bordoli, R. S.; Sedgwick, R. D.; Tyler, A. N. Fast atom bombardment mass spectrometry of the angiotensin peptides. *Biomed Mass Spectrom* **1982**, *9* (5), 208-214. DOI: 10.1002/bms.1200090506 From NLM Medline.
(35) Cotter, R. J. Plasma desorption mass spectrometry: coming of age. *Anal Chem* **1988**, *60* (13), 781A-793A. DOI: 10.1021/ac00164a002 From NLM Medline.
(36) Craig, A. G.; Engstrom, A.; Bennich, H.; Kamensky, I. Proceedings of the 35th ASMS Conference on Mass Spectrometry and Allied Topics; Denver, CO, 1987, pp. 528-29.
(37) Nelson, R. W.; Dogruel, D.; Willimas, P. Mass Determination of Human Immunoglobulin IgM Using Matrix-assisted Laser Desorption/Ionization Time-of-flight Mass Spectrometry *Rapid Communications in Mass Spectrometry* **1994**, *8*, 627-631. DOI: https://doi.org/10.1002/rcm.1290080811.
(38) Loo, J. A.; Udseth, H. R.; Smith, R. D. Peptide and Protein Analysis by Electrospray Ionization Mass Spectrometry and Capillary Electrophoresis-Mass Spectrometry *Analytical Biochemistry* **1989**, *179*, 404-412. DOI: https://doi.org/10.1016/0003-2697(89)90153-X.
(39) van Berkel, G. J.; Glish, G. L.; McLuckey, S. A. Electrospray Ionization Combined with Ion Trap Mass Spectrometry. *Analytical Chemistry* **1990**, *62*, 1284-1295. DOI: https://pubs.acs.org/doi/pdf/10.1021/ac00212a016.
(40) Ganem, B.; Li, Y.-T.; Henion, J. D. Detection of Noncovalent Receptor-Ligand Complexesby Mass Spectrometry. *Journal of the American Chemical Society* **1991**, *113*, 6294-6296. DOI: https://pubs.acs.org/doi/epdf/10.1021/ja00016a069.
(41) Katta, V.; Chait, B. T. Observation of the heme-globin complex in native myoglobin by electrospray-ionization mass spectrometry. *Journal of the American Chemical Society* **1991**, *113* (22), 5834-8535. DOI: doi.org/10.1021/ja00022a058.
(42) Chernushevich, I. V.; Ens, W.; Standing, K. G. Eletrospray Ionisation Time-of-Flight Mass Spectrometry, Electrospray Ionisation Mass Spectrometry, Chapter 6. Editor Richard B. Cole. **1997**.
(43) Krutchinsky, A. N.; Chernushevich, I. V.; Spicer, V. L.; Ens, W.; Standing, K. G. Collisional damping interface for an electrospray ionization time-of-flight mass spectrometer. *Journal of the American Society for Mass Spectrometry* **1998**, *9* (6), 569–579.

(44) Schwartz, B. L.; Bruce, J. E.; Anderson, G. A.; Hofstadler, S. A.; Rockwood, A. L.; Smith, R. D.; Chilkoti, A.; Stayton, P. S. Dissociation of tetrameric ions of noncovalent streptavidin complexes formed by electrospray ionization. *J Am Soc Mass Spectrom* **1995**, *6* (6), 459-465. DOI: 10.1016/1044-0305(95)00191-F From NLM PubMed-not-MEDLINE.
(45) Biemann, K. Contributions of mass spectrometry to peptide and protein structure. *Biomed Environ Mass Spectrom* **1988**, *16* (1-12), 99-111. DOI: 10.1002/bms.1200160119 From NLM Medline.
(46) Loo, J. A. Stability of Gas Phase Noncovalent Protein Complexes Produced by Electrospray Ionization. *Proceedings of the 47th ASMS Conference on Mass Spectrometry and Allied Topics, Dallas, Texas, June 13 - 17, 1999*.
(47) Loo, J. A. Observation of large subunit protein complexes by electrospray ionisation mass spectrometry. *Journal of Mass Spectrometry* **1995**, *30* (1), 180-183. DOI: https://analyticalsciencejournals.onlinelibrary.wiley.com/doi/10.1002/jms.1190300127.
(48) Wilm, M.; Mann, M. Analytical properties of the nanoelectrospray ion source. *Anal Chem* **1996**, *68* (1), 1-8.
(49) Wilm, M.; Mann, M. Electrospray and Taylor-Cone theory, Dole's beam of macromolecules at last? . *International Journal of Mass Spectrometry and Ion Process* **1994**, *136*, 167-180. DOI: doi.org/10.1016/0168-1176(94)04024-9.
(50) Morris, H. R.; Paxton, T.; Dell, A.; Langhorne, J.; Berg, M.; Bordoli, R. S.; Hoyes, J.; Bateman, R. H. High sensitivity collisionally-activated decomposition tandem mass spectrometry on a novel quadrupole/orthogonal-acceleration time-of-flight mass spectrometer. *Rapid Commun Mass Spectrom* **1996**, *10* (8), 889-896. DOI: 10.1002/(SICI)1097-0231(19960610)10:8<889::AID-RCM615>3.0.CO;2-F.
(51) Morris, M.; Brown, J.; Green, M.; Wildgooose, J.; Pringle, S.; Giles, K. The History of Time-of-Flight Mass Spectrometry at VG - Micromass - Waters. **2014**, *https://www.asms.org/docs/default-source/history-posters/15_vendor-history_waters_tof_updated-file.pdf?sfvrsn=856573c3_0*.
(52) Rostom, A. A.; Robinson, C. V. Detection of the Intact GroEL Chaperonin Assembly by Mass Spectrometry. *Journal of the American Chemical Society* **1999**, *121*, 4718-4719.
(53) Rostom, A. A.; Fucini, P.; Benjamin, D. R.; Juenemann, R.; Nierhaus, K. H.; Hartl, F. U.; Dobson, C. M.; Robinson, C. V. Detection and selective dissociation of intact ribosomes in a mass spectrometer. *Proc Natl Acad Sci U S A* **2000**, *97* (10), 5185-5190. DOI: 10.1073/pnas.97.10.5185.
(54) Tito, M. A.; Tars, K.; Valegard, K.; Hajdu, J.; C.V., R. Electrospray Time-of-Flight Mass Spectrometry of the Intact MS2 Virus Capsid. *Journal of the American Chemical Society* **2000**, *122*, 3550-3551. DOI: https://pubs.acs.org/doi/10.1021/ja993740k.
(55) Rose, R. J.; Damoc, E.; Denisov, E.; Makarov, A.; Heck, A. J. High-sensitivity Orbitrap mass analysis of intact macromolecular assemblies. *Nat Methods* **2012**, *9* (11), 1084-1086. DOI: 10.1038/nmeth.2208.
(56) Belov, M. E.; Damoc, E.; Denisov, E.; Compton, P. D.; Horning, S.; Makarov, A. A.; Kelleher, N. L. From protein complexes to subunit backbone fragments: a multi-stage approach to native mass spectrometry. *Anal Chem* **2013**, *85* (23), 11163-11173. DOI: 10.1021/ac4029328.
(57) Campuzano, I. D. G.; Nshanian, M.; Spahr, C.; Lantz, C.; Netirojjanakul, C.; Li, H.; Wongkongkathep, P.; Wolff, J. J.; Loo, J. A. High Mass Analysis with a Fourier Transform Ion Cyclotron Resonance Mass Spectrometer: From Inorganic Salt Clusters to Antibody Conjugates and Beyond. *J Am Soc Mass Spectrom* **2020**, *31* (5), 1155-1162. DOI: 10.1021/jasms.0c00030.
(58) Desligniere, E.; Yin, V. C.; Ebberink, E.; Rolland, A. D.; Barendregt, A.; Worner, T. P.; Nagornov, K. O.; Kozhinov, A. N.; Fort, K. L.; Tsybin, Y. O.; et al. Ultralong transients enhance sensitivity and resolution in Orbitrap-based single-ion mass spectrometry. *Nat Methods* **2024**, *21* (4), 619-622. DOI: 10.1038/s41592-024-02207-8 From NLM Medline. Walker, T. E.; Shirzadeh, M.; Sun, H. M.; McCabe, J. W.; Roth, A.; Moghadamchargari, Z.; Clemmer, D. E.; Laganowsky, A.; Rye, H.; Russell, D. H. Temperature Regulates Stability, Ligand Binding (Mg(2+) and ATP), and Stoichiometry of GroEL-GroES Complexes. *J Am Chem Soc* **2022**, *144* (6), 2667-2678. DOI: 10.1021/jacs.1c11341 From NLM Medline. Zhou, M.; Jones, C. M.;

Wysocki, V. H. Dissecting the large noncovalent protein complex GroEL with surface-induced dissociation and ion mobility-mass spectrometry. *Anal Chem* **2013**, *85* (17), 8262-8267. DOI: 10.1021/ac401497c From NLM Medline. Walker, T.; Sun, H. M.; Gunnels, T.; Wysocki, V.; Laganowsky, A.; Rye, H.; Russell, D. Dissecting the Thermodynamics of ATP Binding to GroEL One Nucleotide at a Time. *ACS Cent Sci* **2023**, *9* (3), 466-475. DOI: 10.1021/acscentsci.2c01065 From NLM PubMed-not-MEDLINE.
(59) Freeke, J.; Robinson, C. V.; Ruotolo, B. T. Residual counter ions can stabilise a large protein complex in the gas phase. *Internations Journal of Mass Spectrometry* **2010**, *298*, 91-98. DOI: doi.org/10.1016/j.ijms.2009.08.001.
(60) Campuzano, I.; Giles, K. *Nanospray Ion Mobility Mass Spectrometry of Selected High Mass Species. Nanoproteomics: Methods and Protocols, Methods in Molecular Biology, (Eds: S. A. Toms, R. Weil), Humana Press, a part of Springer Science+Business Media, LLC, New York* **2011**, *790*, 57-70.
(61) Sobott, F.; Robinson, C. V. Characterising electrosprayed biomolecules using tandem-MS-the noncovalent GroEl chaperonin assembly. *Internation journal of mass spectrometry* **2004**, *236*, 25-32.
(62) Fenn, J. B.; Mann, M.; Meng, C. K.; Wong, S. F.; Whitehouse, C. M. Electrospray ionization for mass spectrometry of large biomolecules. *Science* **1989**, *246* (4926), 64-71.
(63) Heck, A. J. R.; van den Heuvel, R. H. H. Investigation of Intact Protein Complexes by Mass Spectrometry. *Mass Spectrometry Reviews* **2004**, *23*, 368-389. DOI: https://doi.org/10.1002/mas.10081.
(64) Hernandez, H.; Robinson, C. V. Determining the stoichiometry and interactions of macromolecular assemblies from mass spectrometry. *Nat Protoc* **2007**, *2* (3), 715-726. DOI: 10.1038/nprot.2007.73.
(65) Heck, A. J. Native mass spectrometry: a bridge between interactomics and structural biology. *Nat Methods* **2008**, *5* (11), 927-933. DOI: 10.1038/nmeth.1265.
(66) Sobott, F.; Hernandez, H.; McCammon, M. G.; Tito, M. A.; Robinson, C. V. A tandem mass spectrometer for improved transmission and analysis of large macromolecular assemblies. *Anal Chem* **2002**, *74* (6), 1402-1407.
(67) Chernushevich, I. V.; Thomson, B. A. Collisional cooling of large ions in electrospray mass spectrometry. *Anal Chem* **2004**, *76* (6), 1754-1760. DOI: 10.1021/ac035406j.
(68) van den Heuvel, R. H.; van Duijn, E.; Mazon, H.; Synowsky, S. A.; Lorenzen, K.; Versluis, C.; Brouns, S. J.; Langridge, D.; van der Oost, J.; Hoyes, J.; Heck, A. J. Improving the performance of a quadrupole time-of-flight instrument for macromolecular mass spectrometry. *Anal Chem* **2006**, *78* (21), 7473-7483. DOI: 10.1021/ac061039a.
(69) Tito, M. A.; Robinson, C. V. Improvements in or relating to microfluidic sample preparation and mass spectrometry. **2000**, WO 2000-GB2625.
(70) Campuzano, I. D. G.; Giles, K. Investigating gas composision on transport and deolvation of high m/z species in the first vacuum stages of a mass spectrometer. https://www.waters.com/webassets/cms/library/docs/720002744en.pdf.
(71) Fenn, J. B. Mass spectrometric implications of high-pressure ion sources. *International Journal of Mass Spectrometry* **2000**, *2000* (1-3), 459-478. DOI: https://www.sciencedirect.com/science/article/pii/S1387380600003286?via%3Dihub.
(72) Schmidt, A.; Bahr, U.; Karas, M. Influence of pressure in the first pumping stage on analyte desolvation and fragmentation in nano-ESI MS. *Anal Chem* **2001**, *73* (24), 6040-6046. DOI: 10.1021/ac010451h From NLM Medline.
(73) Tahallah, N.; Pinkse, M.; Maier, C. S.; Heck, A. J. The effect of the source pressure on the abundance of ions of noncovalent protein assemblies in an electrospray ionization orthogonal time-of-flight instrument. *Rapid Commun Mass Spectrom* **2001**, *15* (8), 596-601. DOI: 10.1002/rcm.275.
(74) Campuzano, I.; Giles, K.; Hughes, C. Mass spectrometers and mass spectrometric methods using cone gases. **2008**, WO 2008102163.

(75) Bagal, D.; Kitova, E. N.; Liu, L.; El-Hawiet, A.; Schnier, P. D.; Klassen, J. S. Gas phase stabilization of noncovalent protein complexes formed by electrospray ionization. *Anal Chem* **2009**, *81* (18), 7801-7806. DOI: 10.1021/ac900611a.
(76) Lee, J.; Reilly, P. T. Limitation of time-of-flight resolution in the ultra high mass range. *Anal Chem* **2011**, *83* (15), 5831-5833. DOI: 10.1021/ac201537b From NLM Medline.
(77) Giles, K.; Williams, J. P.; Campuzano, I. Enhancements in travelling wave ion mobility resolution. *Rapid Commun Mass Spectrom* **2011**, *25* (11), 1559-1566. DOI: 10.1002/rcm.5013.
(78) Zhong, Y.; Hyung, S. J.; Ruotolo, B. T. Characterizing the resolution and accuracy of a second-generation traveling-wave ion mobility separator for biomolecular ions. *Analyst* **2011**, *136* (17), 3534-3541. DOI: 10.1039/c0an00987c.
(79) Giles, K.; Pringle, S. D.; Worthington, K. R.; Little, D.; Wildgoose, J. L.; Bateman, R. H. Applications of a travelling wave-based radio-frequency-only stacked ring ion guide. *Rapid Commun Mass Spectrom* **2004**, *18* (20), 2401-2414. DOI: 10.1002/rcm.1641.
(80) Collings, B. A.; Douglas, D. J. An extended mass range quadrupole for electrospray mass spectrometry. *International Journal of Mass Spectrometry and Ion Processes* **1997**, *162* (1-3), 121-127. DOI: https://www.sciencedirect.com/science/article/pii/S0168117696044783?via%3Dihub.
(81) Labastie, P.; Doy, M. A high mass range quadrupole spectrometer for cluster studies. *International Journal of Mass Spectrometry and Ion Processes* **1989**, *91* (2), 105-112. DOI: https://www.sciencedirect.com/science/article/pii/0168117689830010?via%3Dihub.
(82) Winger, B. E.; Light-Wahl, K. J.; Ogorzalek Loo, R. R.; Udseth, H. R.; Smith, R. D. Observation and implications of high mass-to-charge ratio ions from electrospray ionization mass spectrometry. *J Am Soc Mass Spectrom* **1993**, *4* (7), 536-545. DOI: 10.1016/1044-0305(93)85015-P.
(83) Douglas, D. J. Linear quadrupoles in mass spectrometry. *Mass Spectrom Rev* **2009**, *28* (6), 937-960. DOI: 10.1002/mas.20249 From NLM PubMed-not-MEDLINE.
(84) Aquilina, J. A.; Benesch, J. L.; Bateman, O. A.; Slingsby, C.; Robinson, C. V. Polydispersity of a mammalian chaperone: mass spectrometry reveals the population of oligomers in alphaB-crystallin. *Proc Natl Acad Sci U S A* **2003**, *100* (19), 10611-10616. DOI: 10.1073/pnas.1932958100.
(85) Uetrecht, C.; Versluis, C.; Watts, N. R.; Roos, W. H.; Wuite, G. J.; Wingfield, P. T.; Steven, A. C.; Heck, A. J. High-resolution mass spectrometry of viral assemblies: molecular composition and stability of dimorphic hepatitis B virus capsids. *Proc Natl Acad Sci U S A* **2008**, *105* (27), 9216-9220. DOI: 10.1073/pnas.0800406105.
(86) Campuzano, I. D.; Li, H.; Bagal, D.; Lippens, J. L.; Svitel, J.; Kurzeja, R. J.; Xu, H.; Schnier, P. D.; Loo, J. A. Native MS Analysis of Bacteriorhodopsin and an Empty Nanodisc by Orthogonal Acceleration Time-of-Flight, Orbitrap and Ion Cyclotron Resonance. *Anal Chem* **2016**, *88* (24), 12427-12436. DOI: 10.1021/acs.analchem.6b03762.
(87) Campuzano, I. D. G. A Research Journey: Over a Decade of Denaturing and Native-MS Analyses of Hydrophobic and Membrane Proteins in Amgen Therapeutic Discovery. *J Am Soc Mass Spectrom* **2023**, *34* (10), 2413-2431. DOI: 10.1021/jasms.3c00175 From NLM Medline.
(88) Jennings, K. R. Collision-Induced Decompositions of Aromatic Molecular Ions *International Journal of Mass Spectrometry and Ion Physics* **1968**, *1*, 227-235. DOI: doi.org/10.1016/0020-7381(68)85002-8.
(89) Schey, K. L.; Kenttamaa, H. I.; Wysocki, V. H.; Cooks, R. G. Low-Energy Collisional Activation of Polyatomic Ions with Different Target Gases *International Journal of Mass Spectrometry and Ion Processes* **1989**, *90*, 71-83.
(90) Green, B. N.; Bordoli, R. S.; Hanin, L. G.; Lallier, F. H.; Toulmond, A.; Vinogradov, S. N. Electrospray ionization mass spectrometric determination of the molecular mass of the approximately 200-kDa globin dodecamer subassemblies in hexagonal bilayer hemoglobins. *J Biol Chem* **1999**, *274* (40), 28206-28212. DOI: 10.1074/jbc.274.40.28206 From NLM Medline.

(91) Ruotolo, B. T.; Giles, K.; Campuzano, I.; Sandercock, A. M.; Bateman, R. H.; Robinson, C. V. Evidence for macromolecular protein rings in the absence of bulk water. *Science* **2005**, *310* (5754), 1658-1661. DOI: 1120177 [pii]

10.1126/science.1120177.
(92) Ruotolo, B. T.; Benesch, J. L.; Sandercock, A. M.; Hyung, S. J.; Robinson, C. V. Ion mobility-mass spectrometry analysis of large protein complexes. *Nat Protoc* **2008**, *3* (7), 1139-1152. DOI: nprot.2008.78 [pii]

10.1038/nprot.2008.78.
(93) Bush, M. F.; Hall, Z.; Giles, K.; Hoyes, J.; Robinson, C. V.; Ruotolo, B. T. Collision cross sections of proteins and their complexes: a calibration framework and database for gas-phase structural biology. *Anal Chem* **2010**, *82* (22), 9557-9565. DOI: 10.1021/ac1022953.
(94) Lorenzen, K.; Versluis, C.; Van Duijn, E.; Van den Heuvel, R.; Heck, A. J. R. Optimizing macromolecular tandem mass spectrometry of large non-covalent complexes using heavy collision gases. *Internation journal of mass spectrometry* **2007**, *268* (2-3), 198-206.
(95) Haynes, W. N., Editor-in-Cheif, Handbook of Chemistry and Physics, 95th Edition (2014-2015)
(96) Kevan, L.; Futrell, J. H. Determination of Collision Rate Constants of Fluorocarbon Ions by Ion Cyclotron Resonance. *Journal of the Chemical Society, Faraday Transactions 2: Molecular and Chemical Physics* **1972**, *68*, 1742-1748. Christophorou, L. G.; Olthoff, J. K. Electron Interactions With c-C4F8. *Jornal of Physical Chemistry Reference Data* **2001**, *30* (2), 450-473.
(97) Campuzano, I. D. G.; Robinson, J. H.; Hui, J. O.; Shi, S. D.; Netirojjanakul, C.; Nshanian, M.; Egea, P. F.; Lippens, J. L.; Bagal, D.; Loo, J. A.; Bern, M. Native and Denaturing MS Protein Deconvolution for Biopharma: Monoclonal Antibodies and Antibody-Drug Conjugates to Polydisperse Membrane Proteins and Beyond. *Anal Chem* **2019**, *91* (15), 9472-9480. DOI: 10.1021/acs.analchem.9b00062.
(98) Humphreys, S. C.; Thayer, M. B.; Campuzano, I. D. G.; Netirojjanakul, C.; Rock, B. M. Quantification of siRNA-Antibody Conjugates in Biological Matrices by Triplex-Forming Oligonucleotide ELISA. *Nucleic Acid Ther* **2019**, *29* (3), 161-166. DOI: 10.1089/nat.2018.0770.
(99) Shi, S.; Li, Y.; Cui, Z.; Yan, Y.; Zhang, X.; Tang, J.; Xiao, S. Recent advances in degradation of the most potent industrial greenhouse gas sulfur hexafluoride. *Chemical Engineering Journal* **2023**, *470*, 144166. DOI: https://doi.org/10.1016/j.cej.2023.144166.
(100) Tamara, S.; den Boer, M. A.; Heck, A. J. R. High-Resolution Native Mass Spectrometry. *Chem Rev* **2022**, *122* (8), 7269-7326. DOI: 10.1021/acs.chemrev.1c00212 From NLM Medline.
(101) Benesch, J. L.; Ruotolo, B. T.; Sobott, F.; Wildgoose, J.; Gilbert, A.; Bateman, R.; Robinson, C. V. Quadrupole-time-of-flight mass spectrometer modified for higher-energy dissociation reduces protein assemblies to peptide fragments. *Anal Chem* **2009**, *81* (3), 1270-1274. DOI: 10.1021/ac801950u.
(102) Fort, K. L.; van de Waterbeemd, M.; Boll, D.; Reinhardt-Szyba, M.; Belov, M. E.; Sasaki, E.; Zschoche, R.; Hilvert, D.; Makarov, A. A.; Heck, A. J. Expanding the structural analysis capabilities on an Orbitrap-based mass spectrometer for large macromolecular complexes. *Analyst* **2018**, *143*, 100-105. DOI: https://doi.org/10.1039/C7AN01629H.
(103) Gault, J.; Donlan, J. A.; Liko, I.; Hopper, J. T.; Gupta, K.; Housden, N. G.; Struwe, W. B.; Marty, M. T.; Mize, T.; Bechara, C.; et al. High-resolution mass spectrometry of small molecules bound to membrane proteins. *Nat Methods* **2016**, *13* (4), 333-336. DOI: 10.1038/nmeth.3771.
(104) Worner, T. P.; Aizikov, K.; Snijder, J.; Fort, K. L.; Makarov, A. A.; Heck, A. J. R. Frequency chasing of individual megadalton ions in an Orbitrap analyser improves precision of analysis in single-molecule mass spectrometry. *Nat Chem* **2022**, *14* (5), 515-522. DOI: 10.1038/s41557-022-00897-1.
(105) Ruotolo, B. T.; Hyung, S. J.; Robinson, P. M.; Giles, K.; Bateman, R. H.; Robinson, C. V. Ion mobility-mass spectrometry reveals long-lived, unfolded intermediates in the dissociation of protein complexes. *Angew Chem Int Ed Engl* **2007**, *46* (42), 8001-8004. DOI: 10.1002/anie.200702161. Hall, Z.; Politis, A.;

Bush, M. F.; Smith, L. J.; Robinson, C. V. Charge-state dependent compaction and dissociation of protein complexes: insights from ion mobility and molecular dynamics. *J Am Chem Soc* **2012**, *134* (7), 3429-3438. DOI: 10.1021/ja2096859.
(106) Mamyrin, B. A. Time-of-flight mass spectrometry (concepts, achievements, and prospects). *International Journal of Mass Spectrometry* **2001**, *206*, 251-266. DOI: https://www.sciencedirect.com/science/article/pii/S1387380600003924?via%3Dihub.
(107) Guilhaus, M. Special feature: Tutorial. Principles and instrumentation in time-of-flight mass spectrometry. Physical and instrumental concepts. *Journal of Mass Spectrometry* **1995**, *30* (11), 1519-1532. DOI: https://doi.org/10.1002/jms.1190301102.
(108) Guilhaus, M.; Mlynski, V.; Selby, D. Perfect Timing: Time-of-flight Mass Spectrometry. *Rapid Communications in Mass Spectrometry* **1997**, *11*, 951-962. DOI: https://analyticalsciencejournals.onlinelibrary.wiley.com/doi/10.1002/(SICI)1097-0231(19970615)11:9%3C951::AID-RCM785%3E3.0.CO;2-H.
(109) Liu, R.; Li, Q.; Smith, L. M. Detection of large ions in time-of-flight mass spectrometry: effects of ion mass and acceleration voltage on microchannel plate detector response. *J Am Soc Mass Spectrom* **2014**, *25* (8), 1374-1383. DOI: 10.1007/s13361-014-0903-2.
(110) Verenchikov, A. N.; Kirillov, S. N.; Vorobyev, A. V.; Makarov, V. V.; Yavor, M. I.; Tonge, R. P.; Langridge, I. J. Multi reflecting TOF MS approaching resolution of 1,000,000 in a wide mass range. *International Journal of Mass Spectrometry* **2025**, *508*, 117395. DOI: https://doi.org/10.1016/j.ijms.2024.117395.
(111) Ipsen, A.; Ebbels, T. M. Prospects for a statistical theory of LC/TOFMS data. *J Am Soc Mass Spectrom* **2012**, *23* (5), 779-791. DOI: 10.1007/s13361-012-0340-z. Ipsen, A.; Ebbels, T. M. Orders of magnitude extension of the effective dynamic range of TDC-based TOFMS data through maximum likelihood estimation. *J Am Soc Mass Spectrom* **2014**, *25* (10), 1824-1827. DOI: 10.1007/s13361-014-0961-5.
(112) Giles, K.; Gilbert, A.; Green, M. R.; Scott, G. Enhancements to the Ion Mobility Performance of a Travelling Wave Separation Device. *Proc. 58th ASMS Conf. Mass spectrometry and Applied Topics, Philadelphia, 2009, TP227* **2009**.
(113) Chambers, A. *Chapter 6. Modern Vacuum Physics, (Taylor & Francis Masters Series in Physics and Astronomy), Chapman & Hall/CRC, Boca Raton, London, New York, Washington DC*.
(114) Dyachenko, A.; Gruber, R.; Shimon, L.; Horovitz, A.; Sharon, M. Allosteric mechanisms can be distinguished using structural mass spectrometry. *Proc Natl Acad Sci U S A* **2013**, *110* (18), 7235-7239. DOI: 10.1073/pnas.1302395110.
(115) Makarov, A. Electrostatic axially harmonic orbital trapping: a high-performance technique of mass analysis. *Anal Chem* **2000**, *72* (6), 1156-1162.
(116) Olsen, J. V.; Schwartz, J. C.; Griep-Raming, J.; Nielsen, M. L.; Damoc, E.; Denisov, E.; Lange, O.; Remes, P.; Taylor, D.; Splendore, M.; et al. A dual pressure linear ion trap Orbitrap instrument with very high sequencing speed. *Mol Cell Proteomics* **2009**, *8* (12), 2759-2769. DOI: 10.1074/mcp.M900375-MCP200.
(117) Second, T. P.; Blethrow, J. D.; Schwartz, J. C.; Merrihew, G. E.; MacCoss, M. J.; Swaney, D. L.; Russell, J. D.; Coon, J. J.; Zabrouskov, V. Dual-pressure linear ion trap mass spectrometer improving the analysis of complex protein mixtures. *Anal Chem* **2009**, *81* (18), 7757-7765. DOI: 10.1021/ac901278y From NLM Medline.
(118) Olsen, J. V.; Macek, B.; Lange, O.; Makarov, A.; Horning, S.; Mann, M. Higher-energy C-trap dissociation for peptide modification analysis. *Nat Methods* **2007**, *4* (9), 709-712. DOI: 10.1038/nmeth1060.
(119) Lange, O.; Damoc, E.; Wieghaus, A.; Makarov, A. Enhanced Fourier transform for Orbitrap mass spectrometry. *International Journal of Mass Spectrometry* **2014**, *369*, 16-22.

(120) Qi, Y.; Thompson, C. J.; Van Orden, S. L.; O'Connor, P. B. Phase correction of Fourier transform ion cyclotron resonance mass spectra using MatLab. *J Am Soc Mass Spectrom* **2011**, *22* (1), 138-147. DOI: 10.1007/s13361-010-0006-7. Kilgour, D. P.; Nagornov, K. O.; Kozhinov, A. N.; Zhurov, K. O.; Tsybin, Y. O. Producing absorption mode Fourier transform ion cyclotron resonance mass spectra with non-quadratic phase correction functions. *Rapid Commun Mass Spectrom* **2015**, *29* (11), 1087-1093. DOI: 10.1002/rcm.7200.
(121) Kilgour, D. P.; Van Orden, S. L. Absorption mode Fourier transform mass spectrometry with no baseline correction using a novel asymmetric apodization function. *Rapid Commun Mass Spectrom* **2015**, *29* (11), 1009-1018. DOI: 10.1002/rcm.7190.
(122) Snijder, J.; van de Waterbeemd, M.; Damoc, E.; Denisov, E.; Grinfeld, D.; Bennett, A.; Agbandje-McKenna, M.; Makarov, A.; Heck, A. J. Defining the stoichiometry and cargo load of viral and bacterial nanoparticles by Orbitrap mass spectrometry. *J Am Chem Soc* **2014**, *136* (20), 7295-7299. DOI: 10.1021/ja502616y.
(123) Snijder, J.; Rose, R. J.; Veesler, D.; Johnson, J. E.; Heck, A. J. Studying 18 MDa virus assemblies with native mass spectrometry. *Angew Chem Int Ed Engl* **2013**, *52* (14), 4020-4023. DOI: 10.1002/anie.201210197.
(124) van de Waterbeemd, M.; Snijder, J.; Tsvetkova, I. B.; Dragnea, B. G.; Cornelissen, J. J.; Heck, A. J. Examining the Heterogeneous Genome Content of Multipartite Viruses BMV and CCMV by Native Mass Spectrometry. *J Am Soc Mass Spectrom* **2016**, *27* (6), 1000-1009. DOI: 10.1007/s13361-016-1348-6.
(125) Uetrecht, C.; Versluis, C.; Watts, N. R.; Wingfield, P. T.; Steven, A. C.; Heck, A. J. Stability and shape of hepatitis B virus capsids in vacuo. *Angew Chem Int Ed Engl* **2008**, *47* (33), 6247-6251. DOI: 10.1002/anie.200802410.
(126) Li, H.; Nguyen, H. H.; Ogorzalek Loo, R. R.; Campuzano, I. D. G.; Loo, J. A. An integrated native mass spectrometry and top-down proteomics method that connects sequence to structure and function of macromolecular complexes. *Nat Chem* **2018**, *10* (2), 139-148. DOI: 10.1038/nchem.2908.
(127) Cho, Y.; Ahmed, A.; Islam, A.; Kim, S. Developments in FT-ICR MS instrumentation, ionization techniques, and data interpretation methods for petroleomics. *Mass Spectrom Rev* **2015**, *34* (2), 248-263. DOI: 10.1002/mas.21438 From NLM Medline.
(128) Shi, S. D.; Hendrickson, C. L.; Marshall, A. G. Counting individual sulfur atoms in a protein by ultrahigh-resolution Fourier transform ion cyclotron resonance mass spectrometry: experimental resolution of isotopic fine structure in proteins. *Proc Natl Acad Sci U S A* **1998**, *95* (20), 11532-11537.
(129) Tolmachev, A. V.; Robinson, E. W.; Wu, S.; Kang, H.; Lourette, N. M.; Pasa-Tolic, L.; Smith, R. D. Trapped-ion cell with improved DC potential harmonicity for FT-ICR MS. *J Am Soc Mass Spectrom* **2008**, *19* (4), 586-597. DOI: 10.1016/j.jasms.2008.01.006 From NLM Medline.
(130) Campuzano, I. D. G.; Netirojjanakul, C.; Nshanian, M.; Lippens, J. L.; Kilgour, D. P. A.; Van Orden, S.; Loo, J. A. Native-MS Analysis of Monoclonal Antibody Conjugates by Fourier Transform Ion Cyclotron Resonance Mass Spectrometry. *Anal Chem* **2018**, *90* (1), 745-751. DOI: 10.1021/acs.analchem.7b03021.
(131) Campuzano, I. D. G.; Li, H.; Bagal, D.; Schnier, P.; Loo, J. A. Membrane Proteins and Complexes: Using an FTMS to "Shake it Off". *Proc. 63rd ASMS Conf. Mass spectrometry and Applied Topics, St Louis, 2015, TOD am 9:10*.
(132) Rosati, S.; Rose, R. J.; Thompson, N. J.; van Duijn, E.; Damoc, E.; Denisov, E.; Makarov, A.; Heck, A. J. Exploring an orbitrap analyzer for the characterization of intact antibodies by native mass spectrometry. *Angew Chem Int Ed Engl* **2012**, *51* (52), 12992-12996. DOI: 10.1002/anie.201206745.
(133) Campuzano, I. D. G.; Lantz, C.; Wei, Y.; Chen, C. C.; Dillon, T.; Spahr, C.; Wu, S.; Kozhinov, A.; Nagornov, K.; Shilov, I.; et al. Absorption Mode FT for Biopharma: Dramatic Improvements in Native-MS and Denatured RPLC-MS Therapeutic Protein Mass Accuracy, Resolution and PTM Characterization. *Proc. 70th ASMS Conf. Mass Spectrometry and Applied Topics, Minneapolis, 2022, Instrumentation: High-Resolution Mass Spectrometry, MOB am*.

(134) Tiquet, M.; La Rocca, R.; Kirnbauer, S.; Zoratto, S.; Van Kruining, D.; Quinton, L.; Eppe, G.; Martinez-Martinez, P.; Marchetti-Deschmann, M.; De Pauw, E.; Far, J. FT-ICR Mass Spectrometry Imaging at Extreme Mass Resolving Power Using a Dynamically Harmonized ICR Cell with 1omega or 2omega Detection. *Anal Chem* **2022**, *94* (26), 9316-9326. DOI: 10.1021/acs.analchem.2c00754.
(135) Giles, K.; Wildgoose, J.; Williams, J. P.; De Cecco, M. Probing the High Mass Transmission Characteristics of a Conjoined Ion Guide Enabled Quadrupole Ion Mobility Time-of-Flight Instrument. Proc. 61st ASMS Conf. Mass spectrometry and pplied Topics, Mineapolis, 2013, ThP087.
(136) Kenny, D.; Gordon, D.; Giles, K. A New Conjoined RF Ion Guide with Increased Ion Transmission for Labile Compounds. Proc. 64th ASMS Conf. Mass Spectrometry and Applied Topics, San Antonio, 2016, TP414. . Wilson, J. W.; Donor, M. T.; Shepherd, S. O.; Prell, J. S. Increasing Collisional Activation of Protein Complexes Using Smaller Aperture Source Sampling Cones on a Synapt Q-IM-TOF Instrument with a Stepwave Source. *J Am Soc Mass Spectrom* **2020**. DOI: 10.1021/jasms.0c00117 From NLM Publisher.
(137) Harrison, J. A.; Pruska, A.; Bittner, P.; Muck, A.; Cooper-Shepherd, D. A.; Zenobi, R. Advancing Cyclic Ion Mobility Mass Spectrometry Methods for Studying Biomolecules: Toward the Conformational Dynamics of Mega Dalton Protein Aggregates. *Anal Chem* **2022**, *94* (36), 12435-12443. DOI: 10.1021/acs.analchem.2c02406 From NLM Medline.
(138) Sokratous, K.; Cooper-Shepherd, D. A.; Ujma, J.; Qu, F.; Giles, K.; Ben-Younis, A.; Hensen, M.; Langridge, J. I.; Gault, J.; Jazayeri, A.; et al. Enhanced Declustering Enables Native Top-Down Analysis of Membrane Protein Complexes using Ion-Mobility Time-Aligned Fragmentation. *J Am Soc Mass Spectrom* **2024**. DOI: 10.1021/jasms.4c00190 From NLM Publisher.
(139) van de Waterbeemd, M.; Fort, K. L.; Boll, D.; Reinhardt-Szyba, M.; Routh, A.; Makarov, A.; Heck, A. J. High-fidelity mass analysis unveils heterogeneity in intact ribosomal particles. *Nat Methods* **2017**, *14* (3), 283-286. DOI: 10.1038/nmeth.4147 From NLM Medline.
(140) Zheng, Y.; Fornelli, L.; Compton, P. D.; Sharma, S.; Canterbury, J.; Mullen, C.; Zabrouskov, V.; Fellers, R. T.; Thomas, P. M.; Licht, J. D.; et al. Unabridged Analysis of Human Histone H3 by Differential Top-Down Mass Spectrometry Reveals Hypermethylated Proteoforms from MMSET/NSD2 Overexpression. *Mol Cell Proteomics* **2016**, *15* (3), 776-790. DOI: 10.1074/mcp.M115.053819 From NLM Medline.
(141) Melani, R. D.; Srzentic, K.; Gerbasi, V. R.; McGee, J. P.; Huguet, R.; Fornelli, L.; Kelleher, N. L. Direct measurement of light and heavy antibody chains using ion mobility and middle-down mass spectrometry. *MAbs* **2019**, *11* (8), 1351-1357. DOI: 10.1080/19420862.2019.1668226 From NLM Medline.
(142) Commandeur, J. Personal Communication: Optimizing Q-ToF Instruments for Native Mass Spectrometry. Loo, J. A.; Heck, A. J. Editorial and Review: 31(st) ASMS Asilomar Conference on Native Mass Spectrometry-Based Structural Biology. *J Am Soc Mass Spectrom* **2017**, *28* (1), 1-4. DOI: 10.1007/s13361-016-1540-8 From NLM PubMed-not-MEDLINE.
(143) Senko, M. W.; Kovtoun, V. V. Ion Transport Device. **2009**, US 7,514,673 B512.
(144) Lai, Y. H.; Wang, Y. S. Advances in high-resolution mass spectrometry techniques for analysis of high mass-to-charge ions. *Mass Spectrom Rev* **2023**, *42* (6), 2426-2445. DOI: 10.1002/mas.21790 From NLM PubMed-not-MEDLINE.
(145) Zhai, Z.; Schoenmakers, P. J.; Gargano, A. F. G. Identification of heavily glycated proteoforms by hydrophilic-interaction liquid chromatography and native size-exclusion chromatography - High-resolution mass spectrometry. *Anal Chim Acta* **2024**, *1304*, 342543. DOI: 10.1016/j.aca.2024.342543 From NLM In-Process.
(146) Murray, K. K. Resolution and Resolving Power in Mass Spectrometry. *J Am Soc Mass Spectrom* **2022**, *33* (12), 2342-2347. DOI: 10.1021/jasms.2c00216 From NLM PubMed-not-MEDLINE.

(147) Zubarev, R. A.; Makarov, A. Orbitrap mass spectrometry. *Anal Chem* **2013**, *85* (11), 5288-5296. DOI: 10.1021/ac4001223 From NLM Medline. Perry, R. H.; Cooks, R. G.; Noll, R. J. Orbitrap mass spectrometry: instrumentation, ion motion and applications. *Mass Spectrom Rev* **2008**, *27* (6), 661-699. DOI: 10.1002/mas.20186 From NLM Medline.
(148) Makarov, A.; Denisov, E.; Kholomeev, A.; Balschun, W.; Lange, O.; Strupat, K.; Horning, S. Performance evaluation of a hybrid linear ion trap/orbitrap mass spectrometer. *Anal Chem* **2006**, *78* (7), 2113-2120. DOI: 10.1021/ac0518811 From NLM PubMed-not-MEDLINE.
(149) Hecht, E. S.; Eluik, S.; Scigelova, M.; Makarov, A. Fundamentals and Advances of Orbitrap Mass Spectrometry. *Encyclopedia of Analytical Chemistry in 2019 by John Wiley & Sons, Ltd.* DOI: 10.1002/9780470027318.a9309.pub2.
(150) Dillon, T. M.; Bondarenko, P. V.; Rehder, D. S.; Pipes, G. D.; Kleemann, G. R.; Ricci, M. S. Optimization of a reversed-phase high-performance liquid chromatography/mass spectrometry method for characterizing recombinant antibody heterogeneity and stability. *J Chromatogr A* **2006**, *1120* (1-2), 112-120. DOI: 10.1016/j.chroma.2006.01.016. Ren, D.; Pipes, G.; Xiao, G.; Kleemann, G. R.; Bondarenko, P. V.; Treuheit, M. J.; Gadgil, H. S. Reversed-phase liquid chromatography-mass spectrometry of site-specific chemical modifications in intact immunoglobulin molecules and their fragments. *J Chromatogr A* **2008**, *1179* (2), 198-204. DOI: 10.1016/j.chroma.2007.11.088. Lippens, J. L.; Egea, P. F.; Spahr, C.; Vaish, A.; Keener, J. E.; Marty, M. T.; Loo, J. A.; Campuzano, I. D. G. Rapid LC-MS Method for Accurate Molecular Weight Determination of Membrane and Hydrophobic Proteins. *Anal Chem* **2018**, *90* (22), 13616-13623. DOI: 10.1021/acs.analchem.8b03843.
(151) Campuzano, I. D. G.; Larriba, C.; Bagal, D.; Schnier, P. D. Ion Mobility and Mass Spectrometry Measurements of the Humanized IgGk NIST Monoclonal Antibody. *ACS Symposium Series* **2015**, *1202*, 75-112. DOI: 10.1021/bk-2015-1202.ch004.
(152) Shaw, J. B.; Brodbelt, J. S. Extending the isotopically resolved mass range of Orbitrap mass spectrometers. *Anal Chem* **2013**, *85* (17), 8313-8318. DOI: 10.1021/ac401634b.
(153) Gadgil, H. S.; Pipes, G. D.; Dillon, T. M.; Treuheit, M. J.; Bondarenko, P. V. Improving mass accuracy of high performance liquid chromatography/electrospray ionization time-of-flight mass spectrometry of intact antibodies. *J Am Soc Mass Spectrom* **2006**, *17* (6), 867-872. DOI: 10.1016/j.jasms.2006.02.023. Srzentic, K.; Fornelli, L.; Tsybin, Y. O.; Loo, J. A.; Seckler, H.; Agar, J. N.; Anderson, L. C.; Bai, D. L.; Beck, A.; Brodbelt, J. S.; et al. Interlaboratory Study for Characterizing Monoclonal Antibodies by Top-Down and Middle-Down Mass Spectrometry. *J Am Soc Mass Spectrom* **2020**, *31* (9), 1783-1802. DOI: 10.1021/jasms.0c00036 From NLM Medline. Campuzano, I. D. G.; Pelegri-O'Day, E. M.; Srinivasan, N.; Lippens, J. L.; Egea, P.; Umeda, A.; Aral, J.; Zhang, T.; Laganowsky, A.; Netirojjanakul, C. High-Throughput Mass Spectrometry for Biopharma: A Universal Modality and Target Independent Analytical Method for Accurate Biomolecule Characterization. *J Am Soc Mass Spectrom* **2022**, *33* (11), 2191-2198. DOI: 10.1021/jasms.2c00138.
(154) McGee, J. P.; Melani, R. D.; Yip, P. F.; Senko, M. W.; Compton, P. D.; Kafader, J. O.; Kelleher, N. L. Isotopic Resolution of Protein Complexes up to 466 kDa Using Individual Ion Mass Spectrometry. *Anal Chem* **2021**, *93* (5), 2723-2727. DOI: 10.1021/acs.analchem.0c03282 From NLM Medline.
(155) Bern, M.; Caval, T.; Kil, Y. J.; Tang, W.; Becker, C.; Carlson, E.; Kletter, D.; Sen, K. I.; Galy, N.; Hagemans, D.; et al. Parsimonious Charge Deconvolution for Native Mass Spectrometry. *J Proteome Res* **2018**, *17* (3), 1216-1226. DOI: 10.1021/acs.jproteome.7b00839.
(156) Dillon, T. M.; Ricci, M. S.; Vezina, C.; Flynn, G. C.; Liu, Y. D.; Rehder, D. S.; Plant, M.; Henkle, B.; Li, Y.; Deechongkit, S.; et al. Structural and functional characterization of disulfide isoforms of the human IgG2 subclass. *J Biol Chem* **2008**, *283* (23), 16206-16215. DOI: 10.1074/jbc.M709988200. Ren, D.; Pipes, G. D.; Hambly, D.; Bondarenko, P. V.; Treuheit, M. J.; Gadgil, H. S. Top-down N-terminal sequencing of Immunoglobulin subunits with electrospray ionization time of flight mass spectrometry. *Anal Biochem* **2009**, *384* (1), 42-48. DOI: 10.1016/j.ab.2008.09.026.

(157) Brown, J. M.; Williams, J. P.; Hoyes, E.; Cooper-Shepherd, D. A.; Lanucara, F.; Denbigh, L.; Morris, M. Factors Affecting Spectral Quality of Monoclonal Antibodies from Time-of-Flight Mass Spectrometers. *Proc. of the 65th ASMS Conf. Mass Spectrometry and Applied Topics, Indianapolis, 2017, TP029*.
(158) Fort, K. L.; van de Waterbeemd, M.; Boll, D.; Reinhardt-Szyba, M.; Belov, M. E.; Sasaki, E.; Zschoche, R.; Hilvert, D.; Makarov, A. A.; Heck, A. J. R. Expanding the structural analysis capabilities on an Orbitrap-based mass spectrometer for large macromolecular complexes. *Analyst* **2017**, *143* (1), 100-105. DOI: 10.1039/c7an01629h.
(159) Olsen, J. V.; de Godoy, L. M.; Li, G.; Macek, B.; Mortensen, P.; Pesch, R.; Makarov, A.; Lange, O.; Horning, S.; Mann, M. Parts per million mass accuracy on an Orbitrap mass spectrometer via lock mass injection into a C-trap. *Mol Cell Proteomics* **2005**, *4* (12), 2010-2021. DOI: 10.1074/mcp.T500030-MCP200.
(160) Syka, J. E.; Coon, J. J.; Schroeder, M. J.; Shabanowitz, J.; Hunt, D. F. Peptide and protein sequence analysis by electron transfer dissociation mass spectrometry. *Proc Natl Acad Sci U S A* **2004**, *101* (26), 9528-9533. DOI: 10.1073/pnas.0402700101

0402700101 [pii].
(161) Frese, C. K.; Altelaar, A. F.; van den Toorn, H.; Nolting, D.; Griep-Raming, J.; Heck, A. J.; Mohammed, S. Toward full peptide sequence coverage by dual fragmentation combining electron-transfer and higher-energy collision dissociation tandem mass spectrometry. *Anal Chem* **2012**, *84* (22), 9668-9673. DOI: 10.1021/ac3025366.
(162) Zubarev, R. A.; Kelleher, N. L.; McLafferty, F. W. Electron Capture Dissociation of Multiply Charged Protein Cations. A Nonergodic Process. *Journal of the American Chemical Society* **1998**, *120* (13), 3265-3266.
(163) Little, D. P.; Speir, J. P.; Senko, M. W.; O'Connor, P. B.; McLafferty, F. W. Infrared multiphoton dissociation of large multiply charged ions for biomolecule sequencing. *Anal Chem* **1994**, *66* (18), 2809-2815.
(164) Futrell, J. H.; MIller, C. D. Tandem Mass Spectrometer for the Study of Ion-Molecule Reactions. *Review of Scientific Instruments* **1968**, *37*, 1521-1526.
(165) McLuckey, S. A.; Glish, G. L.; Van Berkel, G. J. Multiple stages of mass spectrometry in a quadrupole ion trap mass spectrometer: prerequisites. *International Journal of Mass Spectrometry and Ion Processes* **1991**, *106*, 213-235. DOI: https://doi.org/10.1016/0168-1176(91)85020-M. Grayson, M. A. Origins of Tandem Mass Spectrometry. *https://www.asms.org/docs/history-posters/tandem-ms-poster-2012.pdf?sfvrsn=39e13d69_2*.
(166) Stiving, A. Q.; VanAernum, Z. L.; Busch, F.; Harvey, S. R.; Sarni, S. H.; Wysocki, V. H. Surface-Induced Dissociation: An Effective Method for Characterization of Protein Quaternary Structure. *Anal Chem* **2019**, *91* (1), 190-209. DOI: 10.1021/acs.analchem.8b05071 From NLM Medline.
(167) Merenbloom, S. I.; Koeniger, S. L.; Valentine, S. J.; Plasencia, M. D.; Clemmer, D. E. IMS-IMS and IMS-IMS-IMS/MS for separating peptide and protein fragment ions. *Anal Chem* **2006**, *78* (8), 2802-2809. DOI: 10.1021/ac052208e. Kemper, P. R.; Dupuis, N. F.; Bowers, M. T. A new, higher resolution, ion mobility mass spectrometer. *International Journal of Mass Spectrometry* **2009**, *287*, 46-57.
(168) Giles, K.; Pringle, S.; Wildgoose, J.; Bateman, R. H. Characterising a Travelling Wave-based Ion Mobility Separator. *Proc. of the 54th ASMS Conf. Mass Spectrometry and Applied Topics, Seattle, 2006, MOF*. Campuzano, I. D. G.; Giles, K. Historical, Current and Future Developments of Travelling Wave Ion Mobility Mass Spectrometry: A Personal Perspective. *Trends in Analytical Chemistry* **2019**, *120*. DOI: doi.org/10.1016/j.trac.2019.115620.
(169) Michelmann, K.; Silveira, J. A.; Ridgeway, M. E.; Park, M. A. Fundamentals of trapped ion mobility spectrometry. *J Am Soc Mass Spectrom* **2015**, *26* (1), 14-24. DOI: 10.1007/s13361-014-0999-4.

(170) Panczyk, E. M.; Lin, Y. F.; Harvey, S. R.; Snyder, D. T.; Liu, F. C.; Ridgeway, M. E.; Park, M. A.; Bleiholder, C.; Wysocki, V. H. Evaluation of a Commercial TIMS-Q-TOF Platform for Native Mass Spectrometry. *J Am Soc Mass Spectrom* **2024**. DOI: 10.1021/jasms.3c00320 From NLM Publisher.
(171) Lermyte, F.; Williams, J. P.; Brown, J. M.; Martin, E. M.; Sobott, F. Extensive Charge Reduction and Dissociation of Intact Protein Complexes Following Electron Transfer on a Quadrupole-Ion Mobility-Time-of-Flight MS. *J Am Soc Mass Spectrom* **2015**, *26* (7), 1068-1076. DOI: 10.1007/s13361-015-1124-z From NLM Medline.
(172) Le Huray, K. I. P.; Worner, T. P.; Moreira, T.; Dembek, M.; Reinhardt-Szyba, M.; Devine, P. W. A.; Bond, N. J.; Fort, K. L.; Makarov, A. A.; Sobott, F. To 200,000 m/z and Beyond: Native Electron Capture ChargeReduction Mass Spectrometry Deconvolves Heterogeneous Signalsin Large Biopharmaceutical Analytes. *ACS Central Science*. DOI: https://pubs.acs.org/doi/full/10.1021/acscentsci.4c00462.
(173) Bhanot, J. S.; Fabijanczuk, K. C.; Abdillahi, A. M.; Chao, H. C.; Pizzala, N. J.; Londry, F. A.; Dziekonski, E. T.; Hager, J. W.; McLuckey, S. A. Adaptation and Operation of a Quadrupole/Time-of-Flight Tandem Mass Spectrometer for High Mass Ion/Ion Reaction Studies. *Int J Mass Spectrom* **2022**, *478*. DOI: 10.1016/j.ijms.2022.116874 From NLM PubMed-not-MEDLINE.
(174) Stephenson, J. L., Jr.; McLuckey, S. A. Simplification of product ion spectra derived from multiply charged parent ions via ion/ion chemistry. *Anal Chem* **1998**, *70* (17), 3533-3544. DOI: 10.1021/ac9802832 From NLM Medline. Abdillahi, A. M.; Lee, K. W.; McLuckey, S. A. Mass Analysis of Macro-molecular Analytes via Multiply-Charged Ion Attachment. *Anal Chem* **2020**, *92* (24), 16301-16306. DOI: 10.1021/acs.analchem.0c04335 From NLM Medline.
(175) Huguet, R.; Mullen, C.; Srzentic, K.; Greer, J. B.; Fellers, R. T.; Zabrouskov, V.; Syka, J. E. P.; Kelleher, N. L.; Fornelli, L. Proton Transfer Charge Reduction Enables High-Throughput Top-Down Analysis of Large Proteoforms. *Anal Chem* **2019**, *91* (24), 15732-15739. DOI: 10.1021/acs.analchem.9b03925.
(176) Lermyte, F.; Konijnenberg, A.; Williams, J. P.; Brown, J. M.; Valkenborg, D.; Sobott, F. ETD allows for native surface mapping of a 150 kDa noncovalent complex on a commercial Q-TWIMS-TOF instrument. *J Am Soc Mass Spectrom* **2014**, *25* (3), 343-350. DOI: 10.1007/s13361-013-0798-3.
(177) Campuzano, I. D. G.; Schnier, P. D. Coupling electrospray corona discharge, charge reduction and ion mobility mass spectrometry: From peptides to large macromolecular protein complexes. *International Journal of Ion Mobility Spectrometry* **2013**, *16*, 51-60. DOI: DOI 10.1007/s12127-013-0120-x.
(178) Ebeling, D. D.; Westphall, M. S.; Scalf, M.; Smith, L. M. Corona discharge in charge reduction electrospray mass spectrometry. *Anal Chem* **2000**, *72* (21), 5158-5161.
(179) Scalf, M.; Westphall, M. S.; Krause, J.; Kaufman, S. L.; Smith, L. M. Controlling charge states of large ions. *Science* **1999**, *283* (5399), 194-197. Scalf, M.; Westphall, M. S.; Smith, L. M. Charge reduction electrospray mass spectrometry. *Anal Chem* **2000**, *72* (1), 52-60.
(180) Fu, L.; Eakins, G. S.; Carlsen, M. S.; McLuckey, S. A. Single-Frequency Ion Parking in a Digital 3D Quadrupole Ion Trap. *Int J Mass Spectrom* **2024**, *503*. DOI: 10.1016/j.ijms.2024.117282 From NLM PubMed-not-MEDLINE.
(181) Fu, L.; Ellin, N. R.; Pizzala, N. J.; Baez Bolivar, E. G.; McLuckey, S. A. Digital Ion Trap Isolation and Mass Analysis of Macromolecular Analytes with Multiply Charged Ion Attachment. *J Am Soc Mass Spectrom* **2024**, *35* (9), 2237-2247. DOI: 10.1021/jasms.4c00292 From NLM Medline.
(182) Schrader, R. L.; Walker, T. E.; Chakravorty, S.; Anderson, G. A.; Reilly, P. T. A.; Russell, D. H. Optimization of a Digital Mass Filter for the Isolation of Intact Protein Complexes in Stability Zone 1,1. *Anal Chem* **2023**, *95* (5), 3062-3068. DOI: 10.1021/acs.analchem.2c05221 From NLM Medline.
(183) Fuerstenau, S. D.; Benner, W. H. Molecular weight determination of megadalton DNA electrospray ions using charge detection time-of-flight mass spectrometry. *Rapid Commun Mass Spectrom* **1995**, *9* (15), 1528-1538. DOI: 10.1002/rcm.1290091513.

(184) Contino, N. C.; Pierson, E. E.; Keifer, D. Z.; Jarrold, M. F. Charge detection mass spectrometry with resolved charge states. *J Am Soc Mass Spectrom* **2013**, *24* (1), 101-108. DOI: 10.1007/s13361-012-0525-5. Contino, N. C.; Jarrold, M. F. Charge detection mass spectrometry for single ions with a limit of detection of 30 charges. *International Journal of Mass Spectrometry* **2013**, *34-347*, 153-159. DOI: https://doi.org/10.1016/j.ijms.2012.07.010.
(185) Elliott, A. G.; Merenbloom, S. I.; Chakrabarty, S.; Williams, E. R. Single Particle Analyzer of Mass: A Charge Detection Mass Spectrometer with a Multi-Detector Electrostatic Ion Trap. *International Journal of Mass Spectrometry* **2017**, *414*, 45-55. DOI: 10.1016/j.ijms.2017.01.007.
(186) Jarrold, M. F. Single-Ion Mass Spectrometry for Heterogeneous and High Molecular Weight Samples. *J Am Chem Soc* **2024**, *146* (9), 5749-5758. DOI: 10.1021/jacs.3c08139 From NLM PubMed-not-MEDLINE.
(187) Hanozin, E.; Harper, C. C.; McPartlan, M. S.; Williams, E. R. Dynamics of Rayleigh Fission Processes in approximately 100 nm Charged Aqueous Nanodrops. *ACS Cent Sci* **2023**, *9* (8), 1611-1622. DOI: 10.1021/acscentsci.3c00323 From NLM PubMed-not-MEDLINE.
(188) Worner, T. P.; Snijder, J.; Bennett, A.; Agbandje-McKenna, M.; Makarov, A. A.; Heck, A. J. R. Resolving heterogeneous macromolecular assemblies by Orbitrap-based single-particle charge detection mass spectrometry. *Nat Methods* **2020**, *17* (4), 395-398. DOI: 10.1038/s41592-020-0770-7.
(189) Kafader, J. O.; Melani, R. D.; Durbin, K. R.; Ikwuagwu, B.; Early, B. P.; Fellers, R. T.; Beu, S. C.; Zabrouskov, V.; Makarov, A. A.; Maze, J. T.; et al. Multiplexed mass spectrometry of individual ions improves measurement of proteoforms and their complexes. *Nature Methods* **2020**, *17* (4), 391-+. DOI: 10.1038/s41592-020-0764-5. Kafader, J. O.; Melani, R. D.; Senko, M. W.; Makarov, A. A.; Kelleher, N. L.; Compton, P. D. Measurement of Individual Ions Sharply Increases the Resolution of Orbitrap Mass Spectra of Proteins. *Anal Chem* **2019**, *91* (4), 2776-2783. DOI: 10.1021/acs.analchem.8b04519 From NLM Medline.
(190) Sage, E.; Sansa, M.; Fostner, S.; Defoort, M.; Gely, M.; Naik, A. K.; Morel, R.; Duraffourg, L.; Roukes, M. L.; Alava, T.; et al. Single-particle mass spectrometry with arrays of frequency-addressed nanomechanical resonators. *Nat Commun* **2018**, *9* (1), 3283. DOI: 10.1038/s41467-018-05783-4 From NLM PubMed-not-MEDLINE.
(191) Sader, J. E.; Gomez, A.; Neumann, A. P.; Nunn, A.; Roukes, M. L. Data-driven fingerprint nanoelectromechanical mass spectrometry. *Nat Commun* **2024**, *15* (1), 8800. DOI: 10.1038/s41467-024-51733-8 From NLM PubMed-not-MEDLINE.
(192) Hanay, M. S.; Kelber, S.; Naik, A. K.; Chi, D.; Hentz, S.; Bullard, E. C.; Colinet, E.; Duraffourg, L.; Roukes, M. L. Single-protein nanomechanical mass spectrometry in real time. *Nat Nanotechnol* **2012**, *7* (9), 602-608. DOI: 10.1038/nnano.2012.119 From NLM Medline.
(193) Volny, M.; Elam, W. T.; Branca, A.; Ratner, B. D.; Turecek, F. Preparative soft and reactive landing of multiply charged protein ions on a plasma-treated metal surface. *Anal Chem* **2005**, *77* (15), 4890-4896. DOI: 10.1021/ac0507136 From NLM Medline.
(194) Ouyang, Z.; Takats, Z.; Blake, T. A.; Gologan, B.; Guymon, A. J.; Wiseman, J. M.; Oliver, J. C.; Davisson, V. J.; Cooks, R. G. Preparing protein microarrays by soft-landing of mass-selected ions. *Science* **2003**, *301* (5638), 1351-1354. DOI: 10.1126/science.1088776 From NLM Medline.
(195) Mikhailov, V. A.; Mize, T. H.; Benesch, J. L.; Robinson, C. V. Mass-selective soft-landing of protein assemblies with controlled landing energies. *Anal Chem* **2014**, *86* (16), 8321-8328. DOI: 10.1021/ac5018327.
(196) Westphall, M. S.; Lee, K. W.; Salome, A. Z.; Lodge, J. M.; Grant, T.; Coon, J. J. Three-dimensional structure determination of protein complexes using matrix-landing mass spectrometry. *Nat Commun* **2022**, *13* (1), 2276. DOI: 10.1038/s41467-022-29964-4. Esser, T. K.; Bohning, J.; Onur, A.; Chinthapalli, D. K.; Eriksson, L.; Grabarics, M.; Fremdling, P.; Konijnenberg, A.; Makarov, A.; Botman, A.; et al. Cryo-EM of

soft-landed beta-galactosidase: Gas-phase and native structures are remarkably similar. *Sci Adv* **2024**, *10* (7), eadl4628. DOI: 10.1126/sciadv.adl4628 From NLM Medline.
(197) Chait, B. T. Mass spectrometry--a useful tool for the protein X-ray crystallographer and NMR spectroscopist. *Structure* **1994**, *2* (6), 465-467. DOI: 10.1016/s0969-2126(00)00047-2 From NLM Medline.
(198) Schultz, G. A.; Corso, T. N.; Prosser, S. J.; Zhang, S. A fully integrated monolithic microchip electrospray device for mass spectrometry. *Anal Chem* **2000**, *72* (17), 4058-4063. DOI: 10.1021/ac000325y.
(199) Haberger, M.; Leiss, M.; Heidenreich, A. K.; Pester, O.; Hafenmair, G.; Hook, M.; Bonnington, L.; Wegele, H.; Haindl, M.; Reusch, D.; Bulau, P. Rapid characterization of biotherapeutic proteins by size-exclusion chromatography coupled to native mass spectrometry. *MAbs* **2016**, *8* (2), 331-339. DOI: 10.1080/19420862.2015.1122150. VanAernum, Z. L.; Busch, F.; Jones, B. J.; Jia, M.; Chen, Z.; Boyken, S. E.; Sahasrabuddhe, A.; Baker, D.; Wysocki, V. H. Rapid online buffer exchange for screening of proteins, protein complexes and cell lysates by native mass spectrometry. *Nat Protoc* **2020**, *15* (3), 1132-1157. DOI: 10.1038/s41596-019-0281-0.
(200) Bailey, A. O.; Han, G.; Phung, W.; Gazis, P.; Sutton, J.; Josephs, J. L.; Sandoval, W. Charge variant native mass spectrometry benefits mass precision and dynamic range of monoclonal antibody intact mass analysis. *MAbs* **2018**, *10* (8), 1214-1225. DOI: 10.1080/19420862.2018.1521131.
(201) Wei, B.; Han, G.; Tang, J.; Sandoval, W.; Zhang, Y. T. Native Hydrophobic Interaction Chromatography Hyphenated to Mass Spectrometry for Characterization of Monoclonal Antibody Minor Variants. *Anal Chem* **2019**, *91* (24), 15360-15364. DOI: 10.1021/acs.analchem.9b04467.
(202) Liu, W.; Jayasekera, H. S.; Sanders, J. D.; Zhang, G.; Viner, R.; Marty, M. T. Online Buffer Exchange Enables Automated Membrane Protein Analysis by Native Mass Spectrometry. *Anal Chem* **2023**, *95* (47), 17212-17219. DOI: 10.1021/acs.analchem.3c02164 From NLM Medline.
(203) Strasser, L.; Fussl, F.; Morgan, T. E.; Carillo, S.; Bones, J. Exploring Charge-Detection Mass Spectrometry on Chromatographic Time Scales. *Anal Chem* **2023**, *95* (40), 15118-15124. DOI: 10.1021/acs.analchem.3c03325 From NLM Medline. Yin, V.; Desligniere, E.; Mokiem, N.; Gazi, I.; Lood, R.; de Haas, C. J. C.; Rooijakkers, S. H. M.; Heck, A. J. R. Not All Arms of IgM Are Equal: Following Hinge-Directed Cleavage by Online Native SEC-Orbitrap-Based CDMS. *J Am Soc Mass Spectrom* **2024**, *35* (6), 1320-1329. DOI: 10.1021/jasms.4c00094 From NLM Medline.
(204) Allen, S. J.; Schwartz, A. M.; Bush, M. F. Effects of polarity on the structures and charge states of native-like proteins and protein complexes in the gas phase. *Anal Chem* **2013**, *85* (24), 12055-12061. DOI: 10.1021/ac403139d. Liko, I.; Hopper, J. T.; Allison, T. M.; Benesch, J. L.; Robinson, C. V. Negative Ions Enhance Survival of Membrane Protein Complexes. *J Am Soc Mass Spectrom* **2016**, *27* (6), 1099-1104. DOI: 10.1007/s13361-016-1381-5.

Graphical Abstract

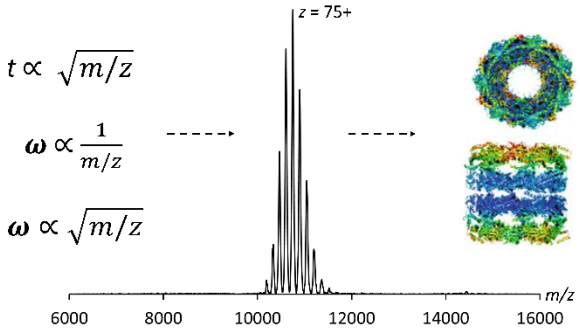

Supporting Information

The Evolution of Mass Spectrometers for High *m/z* Biological Ion Formation, Transmission, Analysis and Detection: A Personal Perspective

Iain D. G. Campuzano[1]* and Joseph A. Loo[2]*

1. Large Molecule Discovery and Research Data Science, Amgen Research, Amgen, Thousand Oaks, California, 91320, USA

2. Department of Chemistry and Biochemistry, and Department of Biological Chemistry, University of California-Los Angeles, Los Angeles, California 90095, USA

*Corresponding authors iainc@amgen.con and jloo@chem.ucla.edu

Supporting Information Contents

Additional Notes and Personal Observations

Noncovalent Complexes become Larger and m/z Values Higher

On this first iteration of the Q-ToF, there was not a direct pressure readout (Pirani gauge) of the source backing region). The hexapole collision cell pressure was carefully optimized from 8.0 x10-4 Pa to 9.0x10-3 Pa, using argon as the collision gas. The source cone voltage was operated at 150 V for optimal desolvation and transmission.

What is High m/z Now?

Inorganic salt clusters such as cesium iodide (CsI) are typically singly charged, therefore the large highly stable clusters such as $[CsI_{43}]Cs^+$, $[CsI_{53}]Cs^+$, $[CsI_{62}]Cs^+$, $[CsI_{72}]Cs^+$, $[CsI_{85}]Cs^+$ that appear high in the *m/z* scale (>m/z 10,000) [1, 2, 3]. Although multiple charged CsI clusters do exit, but at lower intensities [2], that was not evident in the earlier work by Amster and Lebrilla. H

Ion Declustering

Finally, depending on the specific protein Mw and stoichiometry, and as long as the acceleration voltage threshold is not exceeded (typically in the collision cell) delustering will increase without subunit ejection and/or fragmentation (GroEL, based on PDB 4V43; $C_{34622}H_{57738}N_{9660}O_{11159}S_{350}$, has 340,587 degrees of freedom, based on 3*N*, allowing for effective translational energy distribution).

Time-of-Flight Optics

This is performed automatically, based on the spectral acquisition range, however, on the Waters Q-ToF, one has the option to specifically select the pusher frequency (down the single μsec granularity) therefore the upper measured flight time. From a personal observation, we have experienced that operating MCP detectors at a higher gain (voltage; Waters Q-ToFs) is advantageous, for high *m/z* detection.

Xenon (Xe) bleeding into the oa-ToF analyzer: this observation was also recently made during the 72nd Annual ASMS conference by Ebberink [4], when performing CD-MS using Xe as the HCD cooling gas.

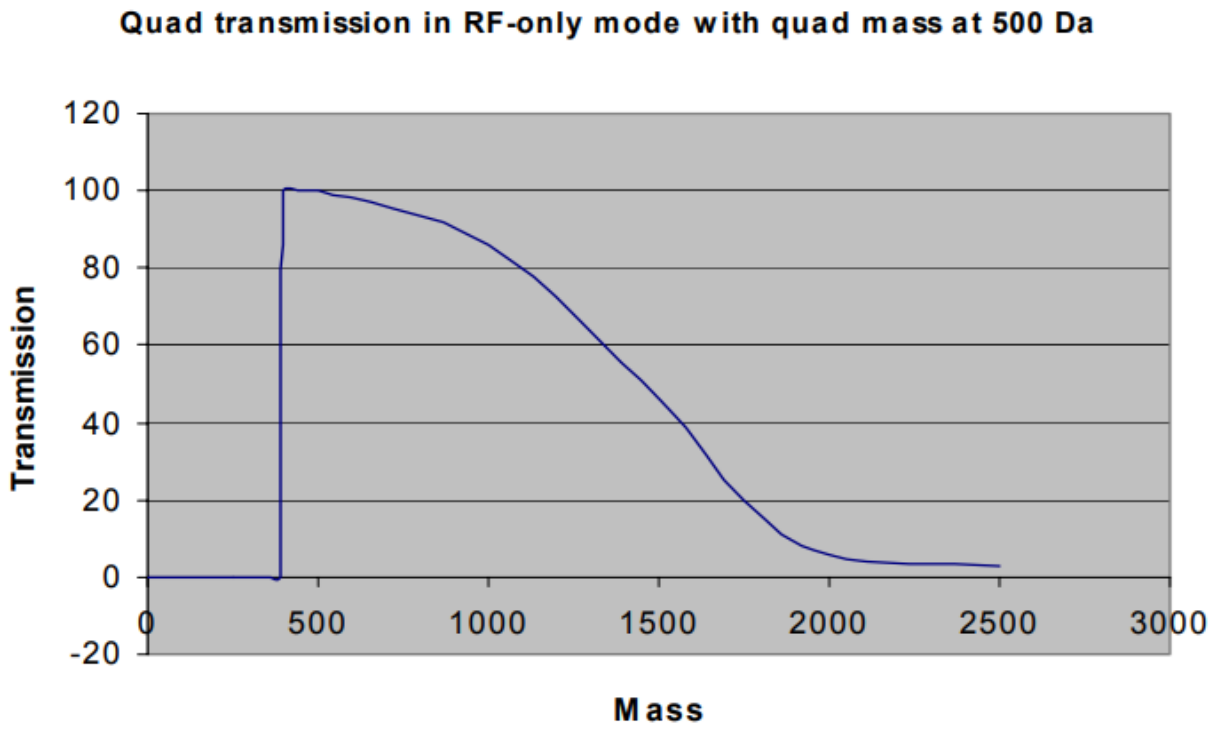

Figure S1. A quadrupole RF-transmission profile plot, reproduced from the Q-ToF Premier Technical Support Notes (32692_1; page 298; Project 910021), with permission from the Waters Corporation, MS Technologies Center, UK. The figure shows that for a set RF value specific for *m/z* 500 transmission, there is a sharp cut off in transmission in the low mass range and a gradual loss of transmission at the high mass range. When performing high *m/z* analyses, its typical to set up an MS Profile, that scans the RF-voltages over a wide *m/z* range, therefore transmitting a wide and high *m/z* range through the quadrupole, subsequent ion optics and in to either the oa-ToF or the Orbitrap analyzer. Scanning the quadrupole RF is also discussed by SCIEX, and can be found here: https://www.sciex.com/support/knowledge-base-articles/how-does-the-quadrupole-transmission-function-in-the-qtof-systems-work_en_us

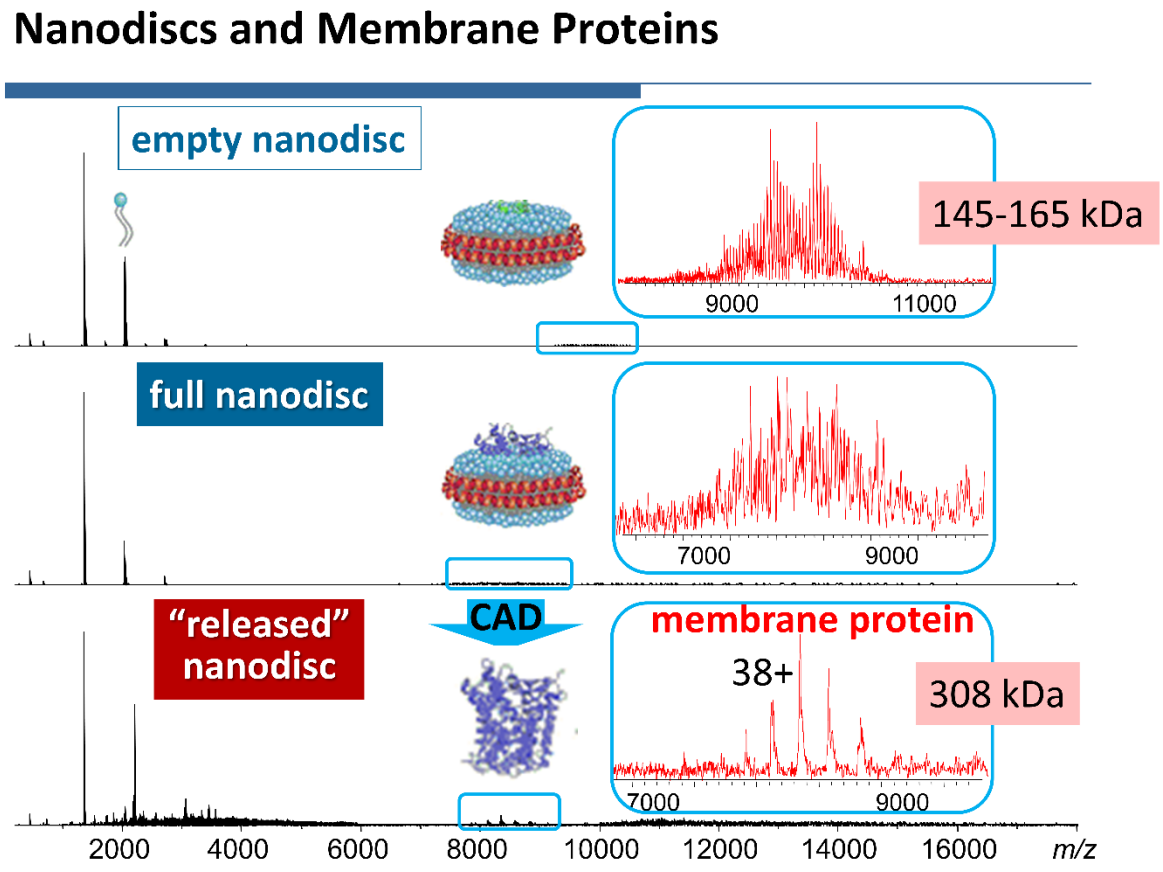

Figure S2. NanoESI analysis of the CYP3A4 loaded nanodisc on a solariX 15 Tesla FT-ICR MS. This data was one of the first tandem-MS acquisitions of a loaded nanodisc, under native-MS conditions (*circa* 2013) as part of the Amgen-UCLA collaboration. The displayed figure is reproduced from the ASMS presentation described in reference [5] and is also discussed in detail in reference [6].

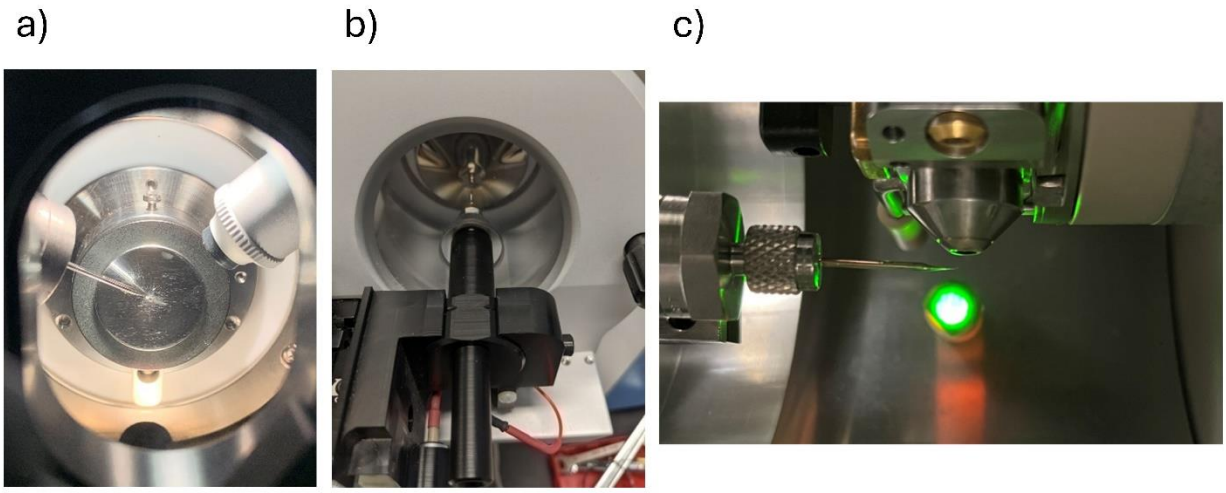

Figure S3. A selection of different nESI sources. a) the UCLA Bruker solariX 15 Tesla FT-ICR source. The nESI needle is mounted at an approximate 45 ° angle to the sampling orifice, which is the direct entrance of the heated transfer capillary. For all the nESI experiments acquired on this 15 Tesla FT-ICR, described by Campuzano and Loo, the capillary was typically set to 100 °C. Upon exist of the ion from the transfer capillary, there is a single orthogonal sampling stage which then directs the ion in thot he first ion funnel; b) the Amgen Orbitrap EMR source. The nESI needle is mounted in an in-line configuration, pointing directly into the source transfer capillary, which is typically set to 200 °C; c) the Micromass/Waters Z-Spray source of the Amgen Synapt G2 HDMS, viewed from above and illuminated from below. The nESI needle is positioned in an orthogonal position next to the Sample Cone. Once the ions enter the Sample Cone there is a second orthogonal sample stage that directs the ions through the Extraction Cone. There is no transfer capillary in the Z-Spray source. For most nESI native-MS experiments, the Z-Spary source is typically operated at ambient temperatures.

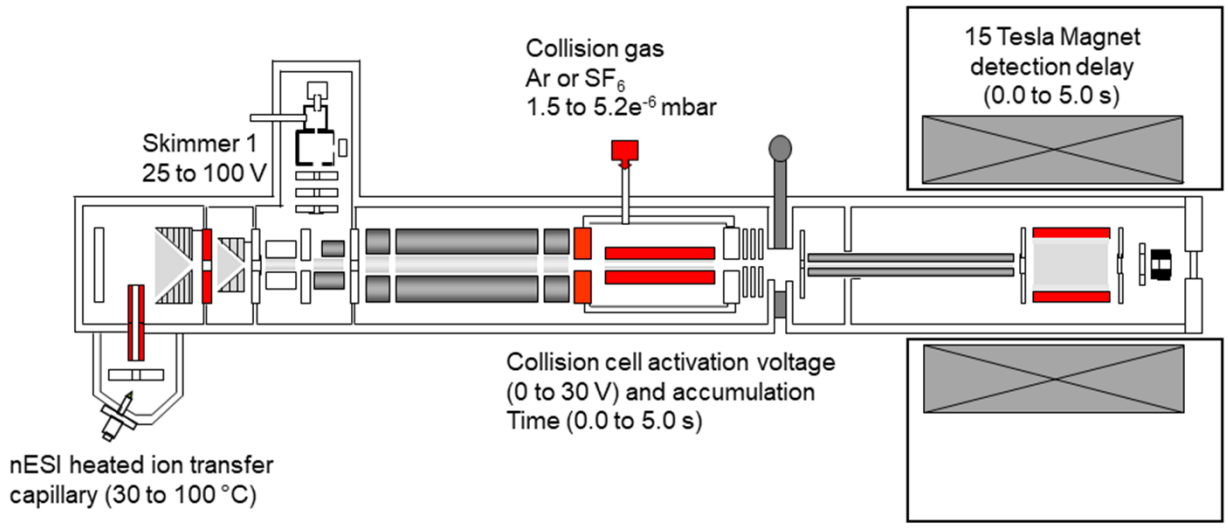

Figure S4. The solariX 15 Tesla FT-ICR schematics. Note the orthogonal ion sampling once the ions leave the heater transfer capillary. Reproduced and modified from reference [3], with permission from the American Chemical Society, Copyright 2020.

Is the Term High Resolution Native-MS Accurate or Appropriate?

If one considers the term "high resolution" for smaller ionic species, then it typically refers to the "narrowness" of the *m/z* peak and therefore the ability to resolve two species. This can be defined by two different and subtly different descriptions, that are described below.

Defined by Equation 1, where resolution is a measure of the peak width at 50% (FWHM) of its height, reproduced from Murray [7]:

$$Resolution\ FWHM = \frac{m/z}{m/z\ width\ at\ FWHM} \qquad (1)$$

Defined by Equation 2, at a specific defined valley, often 10%, whereby two adjacent ions can be separated, based on the MS instrument resolving power, reproduced from Murray [7]:

$$Resolving\ Power = \frac{m/z}{delta\ m/z} \qquad (2)$$

Where delta *m/z* refers to two adjacent peaks on the *m/z* scale that are resolved at 10% valley.

Future Instrument Developments

Native-MS and high *m/z* analysis has become much more routine, useable and accessible due to the development of ESI [8 9] enabling generation of gas-phase native-like biological ions, subsequent detection and exquisite characterization by the MS technologies described herein. MS instrumentation also offers multiple fragmentation techniques, such as electron ionization, collision induced dissociation (CID [10]), higher-energy collision induced dissociation (HCD [11]), electron transfer dissociation (ETD [12]), electron transfer higher-energy collision induced dissociation (EThcD [13]) electron capture dissociation (ECD [14]), infrared multiphoton dissociation (IRMPD [15]) and ultraviolet photo dissociation.[16] to further characterize ions, as a function of tandem-MS [17] or multiple stages of MS (MS^n [18]) and surface induced dissociation [19]. We argue that for high *m/z* and native-MS analyses, all of the above fragmentation methods and ion mobility capabilities such as drift tube [20], travelling wave [2, 21] and trapped ion mobility [22 23], have been enabled by ESI, and benefitted from the source and detector modifications described above, therefore will not be described further.

m/z	**Orbitrap UHMR Resolution (FWHM)**		
400	**25000**	**50000**	**100000**
800	17730	35461	70922
1600	12575	25150	50299
3200	8918	17837	35673
6400	6325	12650	25300
12800	4486	8972	17943
	solariX 15 Tesla FT-ICR Transient Size		
	256k	**512k**	**1M**
m/z	**Resolution**		
400	49000	98000	200000
800	24500	49000	100000
1600	12250	24500	50000
3200	6125	12250	25000
6400	3062	6125	12500
12800	1531	3063	6250

Table S1. A theoretical resolution comparison between the Orbitrap UHMR and the solariX 15 Tesla FT-ICR MS instruments. The Orbitrap and FT-ICR resolution reduces as a function of the square root of the *m/z* and the inverse of the *m/z*, respectively.

a)

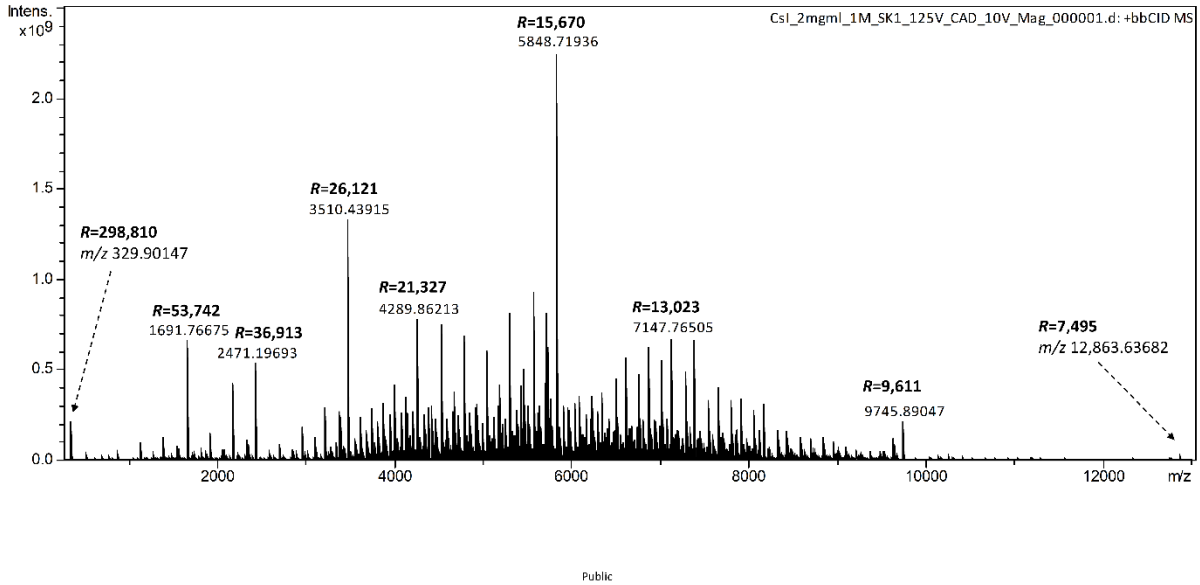

Public

b)

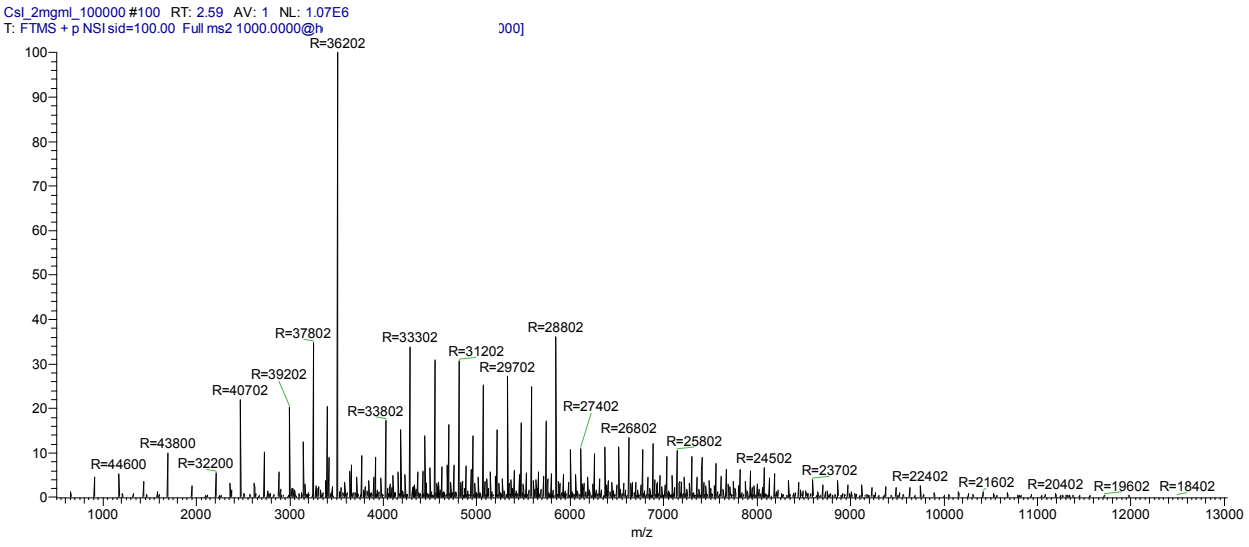

Figure S5. Comparisons of CsI acquired on the a) solariX 15 Tesla FT-ICR, operating at a 1M transient size, equating to a resolution value of 200,000 at *m/z* 400, and b) the Orbitrap UHMR operating at an instrument resolution of 100,000 at *m/z* 400. As can be seen, *m/z* peak width FWHM resolution reduces on the FT-ICR as a function of $(m/z)^{-1}$ and on the Orbitrap, as a function of $(m/z)^{1/2}$.

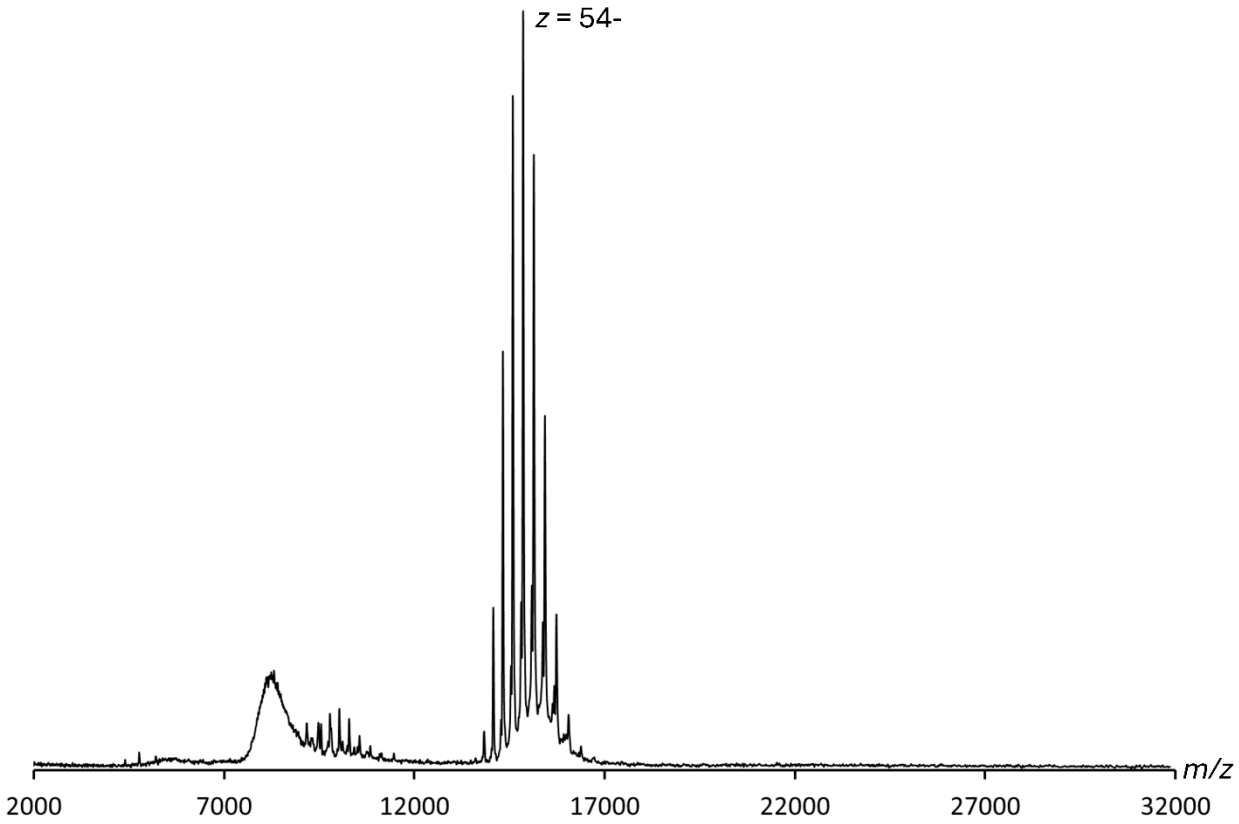

Figure S6. GroEL (5 μM, 200 mM ammonium acetate) analyzed by negative polarity nESI, using a Synapt G1 Q-ToF mass spectrometer (Waters Corporation, MS Technologies, UK). Reproduced and modified from reference [24], with permission from the American Chemical Society, Copyright 2019.

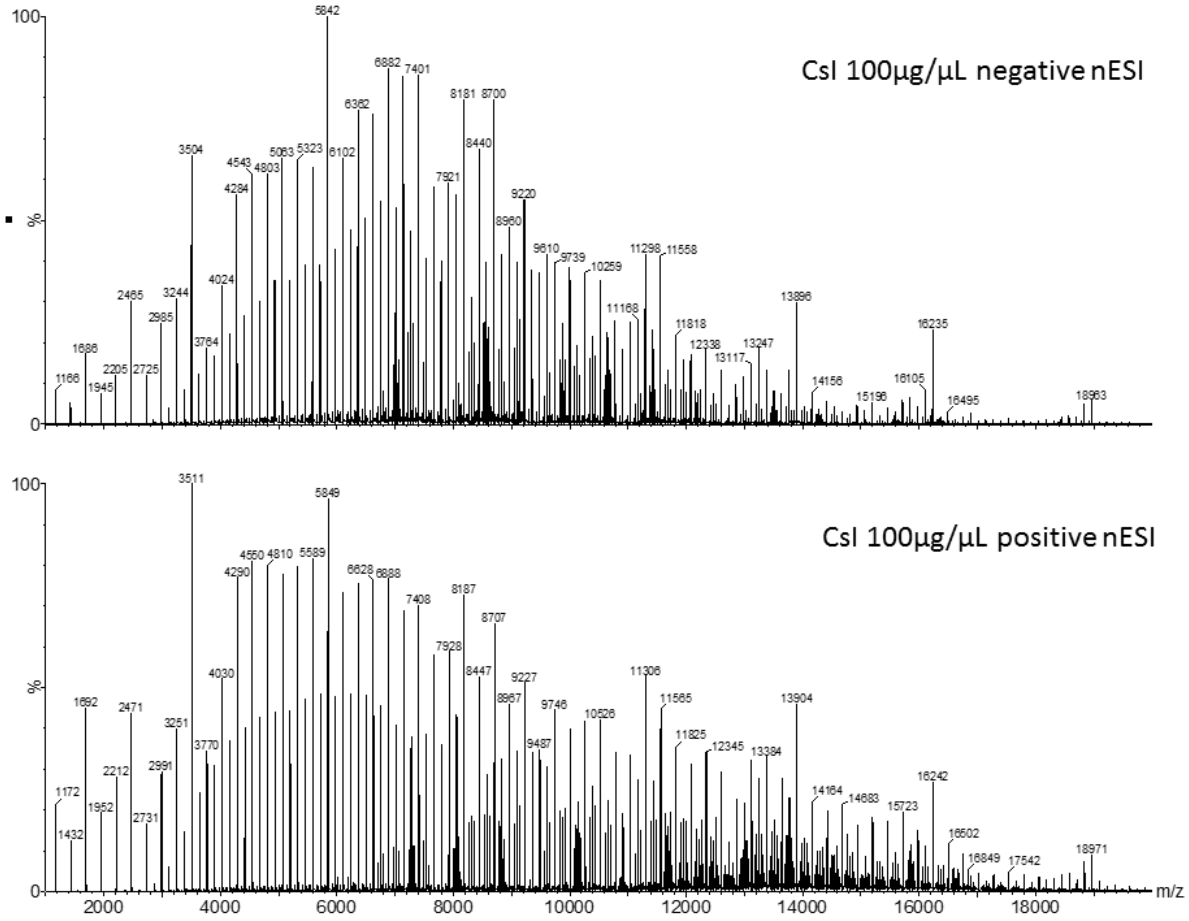

Figure S7. A comparison of positive and negative mode nESI CsI (100 µg/µL, 50% v/v acetonitrile) acquisitions, performed on a Synapt G1 Q-ToF mass spectrometer (Waters Corporation, MS Technologies, UK). Reproduced from reference [24], with permission from the American Chemical Society, Copyright 2019.

References

(1) Sobott, F.; Hernandez, H.; McCammon, M. G.; Tito, M. A.; Robinson, C. V. A tandem mass spectrometer for improved transmission and analysis of large macromolecular assemblies. *Anal Chem* **2002**, *74* (6), 1402-1407. Galhena, A. S.; Jones, C. M.; Wysocki, V. H. Influence of cluster size and ion activation method on the dissociation of cesium iodide clusters. *International Journal of Mass Spectrometry* **2009**, *287*, 105-113.

(2) Campuzano, I.; Giles, K. *Nanospray Ion Mobility Mass Spectrometry of Selected High Mass Species. Nanoproteomics: Methods and Protocols, Methods in Molecular Biology, (Eds: S. A. Toms, R. Weil), Humana Press, a part of Springer Science+Business Media, LLC, New York* **2011**, *790*, 57-70.

(3) Campuzano, I. D. G.; Nshanian, M.; Spahr, C.; Lantz, C.; Netirojjanakul, C.; Li, H.; Wongkongkathep, P.; Wolff, J. J.; Loo, J. A. High Mass Analysis with a Fourier Transform Ion Cyclotron Resonance Mass Spectrometer: From Inorganic Salt Clusters to Antibody Conjugates and Beyond. *J Am Soc Mass Spectrom* **2020**, *31* (5), 1155-1162. DOI: 10.1021/jasms.0c00030.

(4) Ebberink, E.; Yin, V. C.; Desligniere, E.; Barendregt, A.; Worner, T. P.; Kozhinov, A.; Nagamov, K.; Ruisinger, A.; Nuebel, M.; Meyer-Berg, H.; et al. Orbitrap CD-MS with Ultra-long Transients Exposes Distinct Ion Behaviour Between Empty and Filled Adeno-associated Virus Particles. *Proc. 72nd ASMS Conf. Mass Spectrometry and Applied Topics, Anaheim, 2024 WOH am 10.10*.

(5) Campuzano, I. D. G.; Li, H.; Bagal, D.; Schnier, P.; Loo, J. A. Membrane Proteins and Complexes: Using an FTMS to "Shake it Off". *Proc. 63rd ASMS Conf. Mass Spectrometry and Applied Topics, St Louis, 2015, TOD am 9:10*.

(6) Campuzano, I. D. G. A Research Journey: Over a Decade of Denaturing and Native-MS Analyses of Hydrophobic and Membrane Proteins in Amgen Therapeutic Discovery. *J Am Soc Mass Spectrom* **2023**, *34* (10), 2413-2431. DOI: 10.1021/jasms.3c00175 From NLM Medline.

(7) Murray, K. K. Resolution and Resolving Power in Mass Spectrometry. *J Am Soc Mass Spectrom* **2022**, *33* (12), 2342-2347. DOI: 10.1021/jasms.2c00216 From NLM PubMed-not-MEDLINE.

(8) Yamashita, M.; Fenn, J. B. Electrospray ion source. Another variation on the free-jet theme. *J Phys Chem* **1984**, *88* (20), 4451-4459.

(9) Yamashita, M.; Fenn, J. B. Negative Ion Production with the Electrospray Ion Source. *Journal of Physical Chemistry* **1984**, *88*, 4671-4675. Fenn, J. B. Electrospray Wings for Molecular Elephants. **https://www.nobelprize.org/prizes/chemistry/2002/fenn/lecture/**.

(10) Jennings, K. R. Collision-Induced Decompositions of Aromatic Molecular Ions *International Journal of Mass Spectrometry and Ion Physics* **1968**, *1*, 227-235. DOI: doi.org/10.1016/0020-7381(68)85002-8.

(11) Olsen, J. V.; de Godoy, L. M.; Li, G.; Macek, B.; Mortensen, P.; Pesch, R.; Makarov, A.; Lange, O.; Horning, S.; Mann, M. Parts per million mass accuracy on an Orbitrap mass spectrometer via lock mass injection into a C-trap. *Mol Cell Proteomics* **2005**, *4* (12), 2010-2021. DOI: 10.1074/mcp.T500030-MCP200.

(12) Syka, J. E.; Coon, J. J.; Schroeder, M. J.; Shabanowitz, J.; Hunt, D. F. Peptide and protein sequence analysis by electron transfer dissociation mass spectrometry. *Proc Natl Acad Sci U S A* **2004**, *101* (26), 9528-9533. DOI: 10.1073/pnas.0402700101010402700101 [pii].

(13) Frese, C. K.; Altelaar, A. F.; van den Toorn, H.; Nolting, D.; Griep-Raming, J.; Heck, A. J.; Mohammed, S. Toward full peptide sequence coverage by dual fragmentation combining electron-transfer and higher-energy collision dissociation tandem mass spectrometry. *Anal Chem* **2012**, *84* (22), 9668-9673. DOI: 10.1021/ac3025366.

(14) Zubarev, R. A.; Kelleher, N. L.; McLafferty, F. W. Electron Capture Dissociation of Multiply Charged Protein Cations. A Nonergodic Process. *Journal of the American Chemical Society* **1998**, *120* (13), 3265-3266.

(15) Little, D. P.; Speir, J. P.; Senko, M. W.; O'Connor, P. B.; McLafferty, F. W. Infrared multiphoton dissociation of large multiply charged ions for biomolecule sequencing. *Anal Chem* **1994**, *66* (18), 2809-2815.
(16) Melani, R. D.; Srzentic, K.; Gerbasi, V. R.; McGee, J. P.; Huguet, R.; Fornelli, L.; Kelleher, N. L. Direct measurement of light and heavy antibody chains using ion mobility and middle-down mass spectrometry. *MAbs* **2019**, *11* (8), 1351-1357. DOI: 10.1080/19420862.2019.1668226.
(17) Futrell, J. H.; MIller, C. D. Tandem Mass Spectrometer for the Study of Ion-Molecule Reactions. *Review of Scientific Instruments* **1968**, *37*, 1521-1526.
(18) McLuckey, S. A.; Glish, G. L.; Van Berkel, G. J. Multiple stages of mass spectrometry in a quadrupole ion trap mass spectrometer: prerequisites. *International Journal of Mass Spectrometry and Ion Processes* **1991**, *106*, 213-235. DOI: https://doi.org/10.1016/0168-1176(91)85020-M. Grayson, M. A. Origins of Tandem Mass Spectrometry. *https://www.asms.org/docs/history-posters/tandem-ms-poster-2012.pdf?sfvrsn=39e13d69_2*.
(19) Stiving, A. Q.; VanAernum, Z. L.; Busch, F.; Harvey, S. R.; Sarni, S. H.; Wysocki, V. H. Surface-Induced Dissociation: An Effective Method for Characterization of Protein Quaternary Structure. *Anal Chem* **2019**, *91* (1), 190-209. DOI: 10.1021/acs.analchem.8b05071 From NLM Medline.
(20) Merenbloom, S. I.; Koeniger, S. L.; Valentine, S. J.; Plasencia, M. D.; Clemmer, D. E. IMS-IMS and IMS-IMS-IMS/MS for separating peptide and protein fragment ions. *Anal Chem* **2006**, *78* (8), 2802-2809. DOI: 10.1021/ac052208e. Kemper, P. R.; Dupuis, N. F.; Bowers, M. T. A new, higher resolution, ion mobility mass spectrometer. *International Journal of Mass Spectrometry* **2009**, *287*, 46-57. Bush, M. F.; Hall, Z.; Giles, K.; Hoyes, J.; Robinson, C. V.; Ruotolo, B. T. Collision cross sections of proteins and their complexes: a calibration framework and database for gas-phase structural biology. *Anal Chem* **2010**, *82* (22), 9557-9565. DOI: 10.1021/ac1022953.
(21) Giles, K.; Pringle, S. D.; Worthington, K. R.; Little, D.; Wildgoose, J. L.; Bateman, R. H. Applications of a travelling wave-based radio-frequency-only stacked ring ion guide. *Rapid Commun Mass Spectrom* **2004**, *18* (20), 2401-2414. DOI: 10.1002/rcm.1641. Giles, K.; Pringle, S.; Wildgoose, J.; Bateman, R. H. Characterising a Travelling Wave-based Ion Mobility Separator. *Proc. 54th ASMS Conf. Mass Spectrometry and Applied Topics, Seattle, 2006, MOF*. Campuzano, I. D. G.; Giles, K. Historical, Current and Future Developments of Travelling Wave Ion Mobility Mass Spectrometry: A Personal Perspective. *Trends in Analytical Chemistry* **2019**, *120*. DOI: doi.org/10.1016/j.trac.2019.115620. Giles, K.; Williams, J. P.; Campuzano, I. Enhancements in travelling wave ion mobility resolution. *Rapid Commun Mass Spectrom* **2011**, *25* (11), 1559-1566. DOI: 10.1002/rcm.5013.
(22) Michelmann, K.; Silveira, J. A.; Ridgeway, M. E.; Park, M. A. Fundamentals of trapped ion mobility spectrometry. *J Am Soc Mass Spectrom* **2015**, *26* (1), 14-24. DOI: 10.1007/s13361-014-0999-4.
(23) Panczyk, E. M.; Lin, Y. F.; Harvey, S. R.; Snyder, D. T.; Liu, F. C.; Ridgeway, M. E.; Park, M. A.; Bleiholder, C.; Wysocki, V. H. Evaluation of a Commercial TIMS-Q-TOF Platform for Native Mass Spectrometry. *J Am Soc Mass Spectrom* **2024**. DOI: 10.1021/jasms.3c00320 From NLM Publisher.
(24) Campuzano, I. D. G.; Robinson, J. H.; Hui, J. O.; Shi, S. D.; Netirojjanakul, C.; Nshanian, M.; Egea, P. F.; Lippens, J. L.; Bagal, D.; Loo, J. A.; Bern, M. Native and Denaturing MS Protein Deconvolution for Biopharma: Monoclonal Antibodies and Antibody-Drug Conjugates to Polydisperse Membrane Proteins and Beyond. *Anal Chem* **2019**, *91* (15), 9472-9480. DOI: 10.1021/acs.analchem.9b00062.